JOURNAL OF GEOPHYSICAL RESEARCH, VOL. 105, NO. B10, PAGES 23,791–23,810, OCTOBER 10, 2000

Existence of continuum complexity in the elastodynamics of repeated fault ruptures

Bruce E. Shaw
Lamont-Doherty Earth Observatory, Columbia University, Palisades, New York

James R. Rice
Department of Earth and Planetary Sciences and Division of Engineering and Applied Sciences
Harvard University, Cambridge, Massachusetts

Abstract. What are the origins of earthquake complexity? The possibility that some aspects of the complexity displayed by earthquakes might be explained by stress heterogeneities developed through the self-organization of repeated ruptures has been suggested by some simple self-organizing models. The question of whether or not even these simple self-organizing models require at least some degree of material heterogeneity to maintain complex sequences of events has been the subject of some controversy. In one class of elastodynamic models, previous work has described complexity as arising on a model fault with completely uniform material properties. Questions were raised, however, regarding the role of discreteness, the relevance of the nucleation mechanism, and special parameter choices, in generating the complexity that has been reported. In this paper, we examine the question of whether or not continuum complexity is achieved under the stringent conditions of continuous loading, and whether the results are similar to previously claimed findings of continuum complexity or its absence. The elastodynamic model that we use consists of a 1-D fault boundary with friction, a steady slowly moving 1-D boundary parallel to the fault, and a 2-D scalar elastic media connecting the two boundaries. The constitutive law used involves a pair of sequential weakening processes, one occurring over a small slip (or velocity) and accomplishing a small fraction of the total strength drop, and the other at larger slip (or velocity) and providing the remaining strength drop. The large-scale process is motivated by a heat weakening instability. Our main results are as follows. (1) We generally find complexity of type I, a broad distribution of large event sizes with nonperiodic recurrence, when the modeled region is very long, along strike, compared to the layer thickness. (2) We find that complexity of type II, with numerous small events showing a power law distribution, is not a generic result but does definitely exist in a restricted range of parameter space. For that, in the slip weakening version of our model, the strength drop and nucleation size in the small slip process must be much smaller than in the large slip process, and the nucleation length associated with the latter must be comparable to layer thickness. This suggests a basis for reconciling different previously reported results. (3) Bulk dispersion appears to be relatively unimportant to the results. In particular, motions on the fault plane are seen to be relatively insensitive to a wide range of changes in the dispersion in the bulk away from the fault, both at long wavelengths and at short wavelengths. In contrast, the fault properties are seen to be very important to the results. (4) Nucleation from slip weakening and time-dependent weakening showed similar large-scale behavior. However, not all constitutive laws are insensitive to all nucleation approximations; those making a model "inherently discrete" and hence grid-dependent, in particular, can affect large scales. (5) While inherent discreteness has been seen to be a source of power law small-event complexity in some fault models, it does not appear to be the cause of the complexity in the attractors examined here, and reported in earlier work, fortuitously in the special parameter range, with the same class of continuum fault models and same or very similar constitutive relations. Continuum homogeneous dynamic complexity does indeed exist, although that includes type II small-event complexity only under restricted circumstances.

1. Introduction

Earthquakes are complex in many ways. Where they occur, when they occur, and what kind of shaking they produce when they finally do occur are just some of the complicated features we would like to understand. A basic, open question is what is the source of the complexity. Are earthquakes complex because fault zones are complicated? Or might there be some underlying cause that would produce complexity even along a completely homogeneous fault?

There is no doubt that material heterogeneities play a major role in producing the complexity displayed by earthquakes. The question is to what extent do dynamic stress heterogeneities, possibly set up even on a smooth fault of

Paper number 2000JB900203.
0148-0227/00/2000JB900203$09.00

uniform properties by the self-organization of repeated ruptures, also produce complexity. A further question, beyond the scope of this paper, is how the two potential sources of complexity, static material heterogeneities and dynamic stress heterogeneities, might interact. Here we focus our attention instead on the dynamics of a uniform fault, examining questions of complexity in this simpler case, where fewer features of the fault have to be specified.

A theoretical description of earthquakes would mean we had a set of equations that behaved like earthquakes. Decades of research have made it clear that elastodynamics provides a sufficient framework for discussing the waves emanating from the earthquake source [*Aki and Richards*, 1980; *Kostrov and Das*, 1988]. The nonunique inverse problem can be done: Given a set of seismic recordings, a set of source motions can be specified that match the set of records. What remains to be resolved are what are the appropriate combinations of fault-like boundaries and constitutive-based boundary conditions on those boundaries (and perhaps nonelastic constitutive properties in the nearby domain), including their possible spatial variations, such that the source motions are produced in the first place. We are beginning to learn how much of the behavior can be captured by the simplest kinds of descriptions, and what features cannot.

Because the simplest description is both easiest to study and offers the most appealing explanation if it is good enough, that is the place to start. A nearly ubiquitous approximation in elastodynamic models has been to consider a planar fault boundary. How much of the essential physics can be captured in this context remains an open question, particularly when fault properties are uniform. But it is our focus here as a beginning.

There is a long history of studying individual elastodynamic ruptures on planar surfaces. Analytic work on simple elastodynamic cracks established fundamental scaling relations for simple geometries, which formed the basis for quantitative seismology of the source [*Kostrov and Das*, 1988; *Aki and Richards*, 1980]. Numerical work of individual elastodynamic ruptures extended that work to more general boundary conditions [*Ida*, 1973; *Andrews*, 1976; *Madariaga*, 1976; *Day*, 1982; *Okubo and Dieterich*, 1984].

Studying individual ruptures, however, contains some of the difficulties of the inverse problem: a lack of uniqueness, and thus constraints. The forward problem, beginning from a partial differential equation, requires three basic ingredients: the bulk equation of motion, the boundary conditions, and the initial conditions. With an individual rupture the initial conditions and boundary conditions are independently specifiable degrees of freedom that combine to produce one outcome.

There is an even deeper problem in applying individual ruptures to the earthquake problem: that of transients. Earthquakes happen on faults over which there have been many, many previous events. There is time, therefore, for the system to evolve beyond whatever arbitrary initial condition it began from to a state which is compatible with the dynamics in the long term. Thus, earthquakes will lie on an attracting subspace, not the huge transient space of all possible initial conditions. This means that there is a deep relationship between the "initial condition" at a later time and the boundary conditions, coupled through the dynamics. That is, if we treat the value of the field at a later time as an initial condition for the future development, not all initial conditions are possible. The boundary conditions and the initial conditions are not, in effect, independently specifiable degrees of freedom for representative, nontransient events.

The problem of a dynamical attractor for studying individual ruptures becomes, instead, a tremendous asset when we study repeated ruptures. When we examine statistical questions of long sequences on the attractor, the beginning initial conditions can become irrelevant. Studying repeated ruptures thus can usefully avoid the question of what the initial conditions are, and can focus attention onto the more relevant dynamic attracting subspace. It is a description of the dynamics of the attractor that earthquakes lie on that our theoretical description aspires to. This is not to say that the study of specific ruptures is not useful (for an interesting example, see *Olsen, et al.* [1997]). Rather, it is that we obtain additional constraints on the forward problem from studying repeated ruptures.

Are attractors of simple elastodynamic systems interesting? *Carlson and Langer* [1989] and *Horowitz and Ruina* [1989] opened up a new way of looking at the problem by demonstrating that one could get a remarkable amount of complexity out of a system without any material irregularities. Examining repeated ruptures in a one-dimensional elastodynamic model [*Burridge and Knopoff*, 1967] with velocity-weakening friction, Carlson and Langer reported a power law distribution of small events and an excess of large events which occurred above the extrapolated small-event rate. Using modern rate and state friction, *Horowitz and Ruina* [1989] found nonperiodic motion developing in a certain parameter range for very long faults in a quasi-static two-dimensional continuum model in which a velocity-strengthening term, becoming important at higher slip rates, was added to the standard velocity-weakening constitutive law to keep the range of maximum to minimum sliding velocity of the order of 10.

The question of whether the elastodynamic models without any material heterogeneities could produce realistic earthquake like behavior led to further examination of the complexity displayed in the simplest models with, among other things, the cycle of small-event activity preceding large events [*Shaw et al.*, 1992] and the moment source spectra [*Shaw*, 1993] being studied. *Rice* [1993], however, noted a peculiar feature of the results up to that time: that the results at the large scales depended on the resolution of the small scales. Noting that grid resolution could make a difference in whether one obtained complex or periodic behavior in the 2-D and 3-D models that he studied with depth-variable rate and state dependent friction (and with static versus wave-mediated calculation of stress transfers), he raised the question of whether this was more generally true, and, in particular, whether "inherent discreteness" was the cause of the complexity being obtained in some of the self-organizing models. Further work with these models confirmed this

way of generating nonperiodic behavior through discreteness [*Ben-Zion and Rice*, 1995, 1997].

To address the question of whether dependence on grid resolution, and thus discreteness, was the origin of the complexity reported in the simple one-dimensional elastodynamic models, a viscous stress dependent on the curvature of the slip rate distribution was added to the velocity-weakening friction in the one-dimensional model, which then stabilized the smallest scales; large-scale behavior independent of the grid resolution was then obtained, and complexity essentially the same as without the regularizing viscous term was seen [*Shaw*, 1994]. The one-dimensional model does not, however, produce the stress concentrations that occur in higher dimensions, and questions persisted as to whether complexity would occur in higher-dimensional models. A two-dimensional model using slip-weakening friction was then studied and shown to produce complexity [*Myers et al.*, 1996; *Langer et al.*, 1996], interestingly, in many respects very similar to the one-dimensional model. Again, a power law distribution of small events with an excess of large events above the extrapolated small-event rate, and independence of the distribution of sizes of events on the grid resolution was obtained, although (we now know) it was not recognized at the time that the numerous small events, reported as being a generic outcome, depended on fortuitous parameter choices. Velocity-weakening friction, with a viscous regularization, was also shown to give similar results in two dimensions [*Shaw*, 1997] with related parameter choices.

The models of *Myers et al.* [1996] and *Shaw* [1997] both included coupling to stably sliding creeping regions, though in different ways. In the model of *Myers et al.* [1996] the coupling was through the bulk, leading to a Klein-Gordon equation. In the model of *Shaw* [1997], it was through a steadily moving boundary, like for the *Horowitz and Ruina* [1989] configuration, but now leading to a wave equation. Nevertheless, the results from the two different long fault geometries were shown to be nearly the same [*Shaw*, 1997]. Other work on two-dimensional elastodynamic models was also done, with different results reported. A different two-dimensional geometry was considered by *Cochard and Madariaga* [1996] and *Nielsen et al.* [1995], who considered a finite fault, which was pinned at the ends in unbreakable barriers. This geometry was limited, however, to short faults, where the fault length was less than the width of the seismogenic zone. Thus the large events in this geometry break or scale with the whole fault length and are controlled by this imposed geometry. Further, since faults are not allowed to grow, stress singularities develop at the unbreakable ends. *Rice and Ben-Zion* [1996] considered a two-dimensional geometry where only the depth direction was retained, with depth-variable properties as in the model of *Rice* [1993], but modeling the slip distribution as if it was the same at every section along strike. Those authors devised a methodology to resolve fully the initially quasi-static nucleation process in space and time, for the first time in such elastodynamic studies, for a plate loading rate that was 9 orders of magnitude less than seismic slip rates. They found no small-event complexity and, indeed, found only periodic events for the constitutive parameters used, although other studies, reported in the same paper, have hinted that modest alterations in the form of the constitutive law (Dieterich versus Ruina form for state evolution) can sometimes give a distribution of large-event sizes.

The existence of complexity in the small events has been the subject of much discussion in the literature. In addition to the different geometries, different frictions have been used, and different results have been obtained. Using a friction with only a time-dependent drop and neither slip nor velocity weakening, *Nielsen et al.* [1995] saw either periodic or nonperiodic events, depending on the timescale of the drop. Using a small time-dependent drop and slip-weakening friction, *Myers et al.* [1996] saw complexity in the small events. Using a state variable friction that evolved with slip- and velocity-weakening effects, *Cochard and Madariaga* [1996] also saw some complexity in the small events, in a particular parameter range, but not generally. Using a laboratory-based friction with a single logarithmic weakening, *Rice and Ben-Zion* [1996] did not see small-event complexity. Using a small time-dependent drop and velocity-weakening friction, *Shaw* [1997] saw complexity in the small events.

These studies have sharpened current discussions on complexity, with recognition that there are two facets to such complexity: (I) a broad distribution of rupture sizes with nonperiodic event occurrence in time, and (II) an at least approximately power law frequency-size distribution, of Gutenberg-Richter type, over some range of small events. We call this second case "small event complexity." Both types of complexity occur for natural fault zones. In the models the results from the different efforts, as briefly summarized above, have varied.

What are the causes of these different results? Is it the geometry of the models? The frictions? The algorithms? One motivation for this work was to try to reconcile these different results. Most especially, we want to eliminate concerns that particular algorithms may be the source of the model results, and we want to establish, under the most stringent conditions, if and when continuum complexity can indeed occur. A further point that we seek to address is, not only the existence of continuum complexity in some part of parameter space, but the range of behaviors in other areas of parameter space. We observe, in particular, a relatively restricted range of parameter space where there are numerous small events showing a power law distribution of sizes. This suggests a basis for reconciling the different reported results, an issue to which we will return.

One concern raised regarding the reported two- dimensional elastodynamic complexity [*Myers et al.*, 1996; *Shaw*, 1997] was the role of the nucleation process in producing events [*Rice and Ben-Zion*, 1996]. In *Myers et al.* [1996], and *Shaw* [1997], an approximation of the nucleation phase was made, for reasons of computational efficiency, whereby a small but rapid time-dependent drop in friction was used to nucleate events. *Cochard and Madariaga* [1996] also used a small initial drop, instantaneously in their case. These initial drops allowed what *Myers et al* [1996] and *Shaw* [1997] interpreted as seismic events to occur at the smallest single

grid resolution scale. Does this matter? *Lapusta and Rice* [1997, 1998] fully resolved the nucleation process and saw no small-event complexity, although they did not study the parameter ranges analogous to the regimes where *Myers et al* [1996] and *Shaw* [1997] saw the small-event complexity. In this paper, we address the question of whether that particular time-dependent nucleation mechanism is important for the resulting large-scale complexity, and show that, in fact, at least in two dimensions, it is not; in particular, we show that the distribution of sizes of events at large scales is insensitive to that simplification of the nucleation process.

Elastodynamic studies [*Ben-Zion and Rice*, 1997] have shown that another type of simplification, at the smaller scales, rendering grid points capable of failing independently of one another, does indeed affect, and complexify, the larger-scale event distribution, at least for the attractor associated with the friction they used. An analogous approximation with the class of constitutive equations that we consider here did not, however, have obvious qualitative effects on the basic complexity of the attractor [*Shaw*, 1994]. Why these different sensitivities to different perturbations, in this case, the discreteness versus continuum limit of the physics at the small length scales? One possible origin is the nature of the attractor: in the former case, the basic attractor was noncomplex, which may be more sensitive to perturbations than the already complex attractor examined in the latter case. Further work would be needed to resolve these questions. In the absence of a general understanding, however, being in the continuum limit is prudent.

We set for ourselves the most stringent conditions to address, definitively, questions of nucleation and discreteness in obtaining complexity: (1) that there be stability at the smallest scales, (2) that it be done in at least two dimensions, (3) that there be a finite loading rate, with (4) stable aseismic sliding occurring at length scales below a critical stiffness during nucleation and (5) dynamic break-out occurring above that critical stiffness, with (6) grid resolution of the critical stiffness scale and (7) independence of the results on grid resolution. Subject to these conditions, one is looking for events being independent of the small loading rate.

The model we use, which meets all the criteria listed above, consists of the Horowitz-Ruina configuration of a two-dimensional scalar elastic bulk, now satisfying the 2-D wave equation, with one boundary that is slowly loaded and a fault on a parallel boundary that is subject to a frictional force [*Shaw*, 1997]. We modify the previously used model in two ways: we make the loading rate finite, and change the friction so the nucleation phase has either a slip-weakening or a velocity-weakening type instability. In order to make the slip weakening consistent with creep and a finite loading rate, we introduce a healing mechanism, similar to a frictional heating mechanism presented by *Shaw* [1995]. We also add a small amount of strengthening to stabilize the smallest scales. It is important to note that the constitutive laws used involve a pair of weakening processes, one occurring over a small slip (or velocity) and accomplishing a small fraction of the total strength drop, the other at larger slip (or velocity) and providing the remaining strength drop. Our main results are summarized in the abstract, and are presented in more detail in the body of the paper.

The rest of the paper is organized as follows. In section 2, we present the model, and discuss the friction used. Section 3 discusses numerical issues and parameter ranges. The results follow in section 4. We conclude in section 5.

We caution that many of the figures are used to delineate the highly restricted parameter range in which type II small-event complexity with power law features is a legitimate model outcome. Casual perusal of the figures could thus lead to the interpretation that such small-event complexity is a ubiquitous model outcome, whereas, at least in this two-dimensional model that is studied, just the opposite is true. Further, there is a plausible rationalization, which we give in section 5, as to why that restricted parameter range might be expected to produce small-event complexity.

2. The Model

The simplified picture of a fault we have in mind, which we will even further simplify, is as follows. The fault is a planar surface on an elastic bulk which is slowly constantly loaded. Friction on the fault plays a central role in the problem. At depth, below the seismogenic zone, there is frictional strengthening, and the fault slides stably, creeping along at the slow plate loading rate. At seismogenic depths, there is frictional weakening, and the fault slides unstably in sudden stick-slip events [*Brace and Byerlee*, 1966; *Tse and Rice*, 1986; *Blanpied et al.*, 1991; *Rice*, 1993]. The coupling of the stuck seismogenic fault to the lower stably sliding creeping region loads the stuck fault. It also ties the displacement field to a reference field, which then constrains the maximum amount of slip when the whole seismogenic depth ruptures in a large event.

To reduce this to a two-dimensional model, we treat the planar surface as a one-dimensional line, connected to a two-dimensional bulk. Here the slip can be interpreted as an average over the seismogenic depth that is variable along strike, like in the *Rice* [1980], *Lehner et al.* [1981], and *Johnson* [1992] 2-D crustal plane models with elastic (rather than Elsasser viscous) coupling to a mantle substrate. We further simplify the bulk by considering only scalar motions. *Myers et al.* [1996] considered the loading to occur in the bulk, giving a Klein-Gordon equation for the bulk elastodynamics. Here, we use the loading geometry of *Shaw* [1997], which places the loading on a boundary parallel to the fault, giving the wave equation for the bulk elastodynamics. The same configuration was analyzed, both quasi-statically and elastodynamically, by *Rice and Ruina* [1983] for the stability of rate- and state-dependent frictional slip, and was used quasi-statically by *Horowitz and Ruina* [1989] to study event sequences. We use the wave equation model here because it can be run on a smaller domain and is thus more computationally efficient. The results that we present in this paper hold in both geometries.

The two-dimensional wave equation model we use is as follows [*Shaw*, 1997]. We use dimensionless variables throughout, to minimize the number of intrinsic parameters.

In the bulk we have

$$\frac{\partial^2 U}{\partial t^2} = \nabla^2 U \,, \tag{1}$$

where U is the displacement field, t is time, and ∇^2 is the two-dimensional Laplacian operator $\nabla^2 = \partial^2/\partial x^2 + \partial^2/\partial y^2$. We will choose x to be the direction along the fault and y to be the direction perpendicular to the fault. As we want to study the intrinsic complexity of the dynamics, we will choose uniform boundary conditions; by studying the most uniform case, which is most likely to give a periodic response, we give a lower bound to the complexity.

The fault is located at $y = 0$, with the boundary condition that the strain is equal to the (dimensionless) frictional traction Φ acting on the surface:

$$\left.\frac{\partial U}{\partial y}\right|_{y=0} = \Phi \,. \tag{2}$$

We will return to a discussion of Φ shortly; first, let us specify the other boundary conditions.

The loading surface is placed parallel to the fault, a fixed distance away. There the displacement field is moved at a slow steady rate. Without loss of generality, we scale all the lengths in the problem to the distance to this loading surface, so it is located at $y = 1$ (so that unit length should be associated, roughly, with the depth of the seismogenic zone):

$$\left.\frac{\partial U}{\partial t}\right|_{y=1} = \nu \,, \tag{3}$$

where $\nu \ll 1$ is the slow plate loading rate.

Along the fault direction, we use periodic boundary conditions:

$$U(x + L_x) = U(x) \,. \tag{4}$$

To complete the description of the model, it remains to specify the constitutive relation between the friction Φ and slip on the fault $U(x, 0, t)$.

2.1. The Friction

All of the nonlinearity in the problem resides in the friction function Φ. A fundamental element leading to ruptures is that the friction Φ weakens, either with increasing slip or slip rate. The friction Φ we use in this paper is chosen so that we can meet the criteria set out earlier. We use it because it contains the basic slip-weakening instability that we wish to study, which has been shown to be important to laboratory measurements of the nucleation phase of friction [*Dieterich*, 1992], and because of its simplicity. The friction that we use also contains a velocity-weakening limit, which we will also examine. We will, however, focus most of our attention on the slip-weakening nucleation. We choose the friction that we use because it is well controlled and has the properties that we wish to study. It does not equally satisfy both authors. One (J.R.R.) believes that, since the results on complexity are not universal, but do depend on parameter ranges, it would be more prudent to use the standard laboratory-based logarithmic rate and state laws, e.g., as by *Rice and Ben-Zion* [1996], with the now standard Arrhenius-based regularization near zero slip rate [*Heslot et al.*, 1994], and with consideration of possible modification (like in *Zheng and Rice* [1998]) for very short asperity lifetimes, at high slip rates, lying beyond the well-studied laboratory regime. The other author (B.E.S.), who builds on a background of work with laws like those adopted, considers them both physically motivated and easy to study numerically.

The equations are based on a modification of a simplified picture of frictional weakening caused by frictional heating [*Shaw*, 1995, 1997]:

$$\Phi = \phi(\frac{\partial S}{\partial t'}, t' \le t) H(\frac{\partial S}{\partial t}) - \eta \nabla_{||}^2 \frac{\partial S}{\partial t} \,. \tag{5}$$

Here $\partial S/\partial t = \partial U/\partial t|_{y=0}$ is the slip rate on the fault, with ϕ depending on the past history of slip. The function H is the antisymmetric step function, with

$$H = \begin{cases} \widehat{\frac{\partial S}{\partial t}} & \frac{\partial S}{\partial t} \neq 0; \\ |H| < 1 & \frac{\partial S}{\partial t} = 0 \,, \end{cases} \tag{6}$$

where $\widehat{\partial S/\partial t}$ is the unit vector in the sliding direction. Thus H represents the stick-slip nature of the friction, being multivalued at zero slip rate.

The parameter η is the strength of the viscous-like boundary dissipation, with $\nabla_{||}^2 = \partial^2/\partial x^2$ being the fault-parallel Laplacian operator. This term is useful for giving stability to the smallest length scales [*Langer and Nakanishi*, 1993; *Shaw*, 1997], although such stability emerges in a natural way without such a term, when the laboratory-based rate and state laws are used [*Rice and Ruina*, 1983].

The history dependent ϕ we examine in this paper is given by

$$\phi = \Phi_0 - \frac{\alpha Q}{1 + \alpha Q} - \Sigma \tag{7}$$

with

$$\frac{\partial Q}{\partial t} = -\gamma Q + |\frac{\partial S}{\partial t}| \,. \tag{8}$$

Here Φ_0 is the threshold value of sticking friction, which, as long as it is large compared to the maximum friction drop, turns out the be an irrelevant parameter in the problem. The variable Q is something like heat; it accumulates with increasing slip rate on the fault and dissipates on a timescale $1/\gamma$. An equivalent integral solution of Q

$$Q(t) = \int_{-\infty}^{t} e^{-\gamma(t-t')} |\frac{\partial S}{\partial t'}| dt' \tag{9}$$

shows that when $1/\gamma$ is large compared to the rupture timescale of unity, Q is just the slip, while when $1/\gamma$ is small, Q rapidly reaches a steady state value of $1/\gamma$ times the slip rate. Thus γ controls the relative amount of slip-weakening versus velocity-weakening effects [*Shaw*, 1995]. This formulation is based on a physical idea which goes back to *Sibson* [1973], whereby frictional heating increases pore fluid temperature, and therefore pressure, thereby reducing

the effective normal stress. The slow heat dissipation slip-weakening limit was solved by *Lachenbruch* [1980] and later discussed by *Rice* [1994]. *Mase and Smith* [1987] considered additional effects of pore volume expansion. The fast dissipation velocity-weakening limit was pointed out by *Shaw* [1995]. The formulation used here is a simplification [*Shaw*, 1997] of the full nonlinear case [*Shaw*, 1995].

The parameter α is the rate of weakening at small Q, which as we will see will turn out to be a crucial parameter controlling the behavior. It has dimensions of inverse length. The denominator $1+\alpha Q$ is used so as to saturate the drop in friction caused by this term at large Q, with the strength drop scaled to unity.

The third term in the friction, Σ, describes the stress drop in going from sticking to sliding friction. We will make a gross simplification of this term and, for simplicity, consider a Σ which has the same form as the second term:

$$\Sigma = \frac{\beta Q}{1+\beta Q/\sigma} \quad . \tag{10}$$

This gives a drop which weakens initially linearly in Q with slope β, and then saturates to a constant stress drop σ at large Q. It is one of our purposes in this paper to show that the manner in which the stress drop σ occurs is not very important; in particular, we will show that a Σ that changes with time instead of Q gives similar results at large scales. The form of Σ that we use is, however, convenient for studying continuum nucleation and stability issues, a subject we will examine in further detail.

Thus the constitutive law contains a pair of sequential weakening processes, which, together, cause a strength drop of $1+\sigma$. One process is active at "large" slips (or velocities, in the velocity-weakening case) of order $1/\alpha$, and involves a strength drop of order unity. The other is active at small slips (velocities), of order $1/(\alpha+\beta)$, and involves a strength drop of σ. We may consider laws with a single weakening process by either setting $\sigma = 0$ in equation (10), in which case Σ vanishes and β is irrelevant, or by setting $\alpha = 0$ (so the total strength drop is σ). Note that all the crustal-scale earthquake modeling discussed above in the context of laboratory-based rate and state friction has used a constitutive law with a single weakening process, associated with slip-dependent state evolution (evolution of the contact population), with the exception of the *Rice* [1996] shear heating model which has an additional, much larger, slip scale for evolution of elevated pore pressure. However, experiments analyzed in the rate/state framework [*Ruina*, 1983] do sometimes suggest a characterization in terms of a pair of widely different state evolution slip distances. Constitutive relations have been written for such cases and shown [*Ruina*, 1983; *Gu et al.*, 1984] to lead to much richer stability results, with possible regimes of stable but chaotic sliding, in single-degree-of-freedom systems.

The concept of a small-scale strength drop σ seems to have emerged in two interpretations in the literature. In this paper, we introduce σ as part of our constitutive description at small slips, and we try to fully model the nucleation process based on strength drop during those small-scale slips (although we later argue that a simplified representation as a rapid but continuous strength drop σ over some timescale, like in *Myers et al.* [1996], is a valid approximation in the cases we have examined).

The other interpretation of σ is as a computational aid, hoped to be unessential to the final results. One then tends to think of the (small) strength drop σ not as a legitimate part of the constitutive description, but rather as a simple way of kicking the system into dynamic motion when a critical stress has been reached. This obviates the time-consuming calculations of modeling the initially slow and aseismic slip that will ultimately make the transition to rapid dynamic motion. Our results suggest considerable caution in such interpretation of the σ concept. A population of small events will be produced, if σ is small enough, which would go out of existence if σ were set to zero (although then the more difficult nucleation calculations would be required). *Cochard and Madariaga* [1996] adopt this second interpretation of σ and study in an appendix how the artifact population of small events, of stress drop scaling with σ, changes in character over several orders of magnitude reduction in σ.

Our present results confirm that event populations with small σ (say, of order 0.01) are distinctly different, at least for small events, than for $\sigma = 0$. Indeed, there are sound theoretical reasons why we should expect a small-event population to exist for any sufficiently small positive σ, but not necessarily to exist when $\sigma = 0$.

Finally, as an aside, throughout the paper we use the dimensionless formulation we have described in this section, as the minimal parameterization it affords is the most convenient environment in which to examine theoretical and numerical questions. To link with observations, however, it is important to be able to go back and forth between dimensionless and dimensional variables. The conversions to do this are therefore given in Appendix A.

2.2. Stability of the Friction

To examine the stability of the model under the friction that we have chosen, we look at the linearized growth of a sinusoidal perturbation and examine the rate of growth as a function of the wavelength of the perturbation. *Rice and Ruina* [1983] derive the stability results for this case, both quasi-statically and dynamically, with a constitutive formulation that is general enough to include equations (5) to (10), but without the viscous second gradient term in (5). Because the stability analysis for the geometry of *Myers et al.* [1996] is easier, and the results are similar to that for the wave equation, we examine the stability for the friction in the Klein-Gordon equation here. In that model, equations (1)-(2) are replaced by

$$\frac{\partial^2 U}{\partial^2 t} = \nabla^2 U - U + \nu t \quad . \tag{11}$$

Consider the growth of the mode δU off of a uniform creeping solution $U = U_0 + \nu t + \delta U$, where $U_0 = \Phi_0 e^{-y}$ just balances the threshold friction, and

$$\delta U = u_1 e^{ikx-\kappa y+\Omega t} \tag{12}$$

with $|u_1| \ll 1$. First, we consider the slip-weakening case

(although a uniform creeping solution strictly makes sense in that case only if $\nu \ll \gamma$, where one requires $\gamma \ll 1$ to be in the slip-weakening regime; see Appendix B for a full treatment). In the limit where $\gamma = 0$, where we have pure slip-weakening, and with $\eta = 0$, the dispersion relation, using (11), (2), and (12), can be calculated to be

$$\Omega(k) = \sqrt{\hat{\alpha}^2 - k^2 - 1}\,, \tag{13}$$

where $\hat{\alpha}$ is the rate of slip weakening at small slip. For our friction (equations (5)-(10)), which weakens at small Q with slope $\alpha + \beta$, we have $\hat{\alpha} = \alpha + \beta$. We see that at long wavelengths the system is unstable for $\hat{\alpha} > 1$, while at short wavelengths it is marginally stable, having zero real growth rate. The critical half wavelength where the system goes unstable occurs at

$$\hat{x} = \frac{\pi}{\sqrt{\hat{\alpha}^2 - 1}} \approx \frac{\pi}{\hat{\alpha}} \quad \hat{\alpha} \gg 1\,. \tag{14}$$

We also see from this that there is a critical amount of slip weakening, $\hat{\alpha} > 1$, which is needed for the long-wavelength instability. We regard this half wavelength as the equivalent, within a factor of near unity, of the "nucleation size" or "coherent slip patch." Other calculations to represent a finite slipping region give a similar expression with prefactors approximately equal to this value.

In Appendix B, we examine stability to perturbations rigorously for arbitrary nonzero γ. We show that nonzero γ introduces a velocity-weakening part, which, in the absence of any other terms, would then lead to an instability at the smallest wavelengths. With a nonzero η, however, the smallest wavelengths are stabilized. We obtain, from a linearized approximation valid for small γ and small η (see Appendix B),

$$\Omega = \pm i\sqrt{k^2 + 1 - \hat{\alpha}^2} + \left(\frac{\hat{\alpha}^2\gamma}{k^2 + 1 - \hat{\alpha}^2} - \hat{\alpha}\eta k^2\right) + O(\gamma^2, \eta^2, \gamma\eta)\,. \tag{15}$$

From this we see that the high wavenumbers are stabilized by η, having $\mathrm{Re}\,\Omega < 0$, when

$$k^2 > \sqrt{\frac{\hat{\alpha}\gamma}{\eta}}\,. \tag{16}$$

Rice and Ruina [1983] show that an alternative dynamic stabilization at high wave number results from the experimentally observed positive variation of strength with slip rate at fixed state (fixed contact population), as embedded in the standard rate/state laws. No similar experimental basis is known for the η term.

Our only other requirement is that in this slip-weakening case we do not want the η term to be affecting things above the nucleation scale (equation (14)). From (15) we then recommend an upper bound on η,

$$\eta < \frac{1}{2\hat{\alpha}^2}\,, \tag{17}$$

to get a slip-weakening dominated nucleation. For this slip-weakening case, to stabilize the small length scales, we could have used a velocity strengthening term, rather than the viscous-like term we used here, and gotten similar results. For the velocity-weakening case, however, a velocity-strengthening term would not have worked without killing the instability altogether, and something like the viscous term is needed. We therefore, in this paper, consider just the viscous-like dissipation term, a stabilizing mechanism which can handle both cases.

For the velocity-weakening case, which occurs when γ is large, the η term provides stability when, approximately,

$$k^2 > \frac{\alpha'}{\eta}\,, \tag{18}$$

where now $\alpha' = (\alpha + \beta)/\gamma$ is the velocity-weakening rate at large γ. Equation (18) provides an upper bound on the critical k in general and becomes exact when $\gamma \gg 1$ and for $4\alpha' < \eta\gamma^2$. This stability criterion comes from noting the transition from weakening to strengthening in (5) at large k for (7), (8), and (10) with large γ.

We will focus our attention in this paper on the slip-weakening case, both because of its more direct relevance to the slip-weakening nucleation believed to be relevant to real earthquakes, and because it has a more straightforward interpretation in terms of length scales. The velocity weakening does, however, provide analogous results, and helps to show how these results might generalize.

We have found conditions for stability along the fault direction. For the numerics, we also need to know how resolved the structure in the fault perpendicular direction needs to be. From the stability analysis we see that we need to know how big κ, the y direction inverse decay scale, is. For slip weakening, $\kappa = \hat{\alpha}$, independent of k. This is, however, the same size as the maximum k that we need to resolve from (13), so the resolution requirements in both directions are roughly equal. For velocity weakening,

$$\kappa = \Omega(\alpha' - \eta k^2)\,. \tag{19}$$

Using the dispersion relation for (11), (2), and (12) gives

$$\Omega^2 = \frac{k^2 + 1}{(\alpha' - \eta k^2)^2 - 1}\,. \tag{20}$$

The singularity in the denominator, which occurs near the nucleation scale $k = \sqrt{\alpha'/\eta}$, tells us that the Fourier mode is not a good approximation of the structure at the nucleation scale. Nonetheless, away from this singularity we can use the expression to find that for k large,

$$\kappa \approx k \tag{21}$$

is the structure of the modes. Thus again we find the same resolution requirements coming from the fault parallel and perpendicular directions.

3. Numerical Simulation

To solve the partial differential equation (11), we discretize the bulk into equal finite rectangular blocks, approx-

imating the spatial derivatives with finite differences, and then solve a set of coupled ordinary differential equations in time. We use a second-order space, first-order time finite difference approximation. Relative to higher-order approximations, this has the disadvantage of introducing more bulk dispersion at the shortest wavelengths [*Alford et al.*, 1974]. It has the advantage, however, of being faster, and therefore of allowing us more resolution along the fault. As we will see, bulk dispersion does not appear to be important in the results that we will examine, so we make the trade-off in favor of higher fault resolution. For more accurate motions away from the fault, higher-order approximations would be preferable [*Olsen et al.*, 1997].

We have solved the finite difference equations using two different algorithms in order to confirm that the results do not depend on the algorithm used. In one algorithm, we used the formulation of *Virieux and Madariaga* [1982], tracking the velocity field and stress field on a staggered grid with a leap frog in time. Boundary conditions on the fault are implemented through a ghost stress layer, with the stress set by either canceling the stress from the bulk in the stuck phase, or being equal to the sliding friction given by equations (5)-(7) in the sliding phase. The boundary conditions are updated after the velocity and stress fields are updated, giving a three-step staggered cycle. In the second algorithm we track the velocity field and the displacement field at the same points. The fault boundary condition is again implemented with a ghost layer, this time displacement, with the strain set by the stress, and the stress calculated in a way analogous to the previous method. This second algorithm is in some ways more primitive, but it allows us to use a fast and efficient way of damping the radiation, a technique which will be useful in studying nucleation processes without having disturbances from previous events. It also allows an independent check on the independence of the results from the algorithm.

All time increments are done explicitly. Time steps are taken small enough to satisfy numerical stability conditions. In the absence of bulk dissipation the time steps are typically two fifths the timescale of the smallest grid resolution (CFL stability condition 0.4) in the slip-weakening case, and one fifth the grid resolution (CFL condition 0.2) in the velocity-weakening case, while with bulk viscous dissipation they are smaller [*Virieux and Madariaga*, 1982; *Alford et al.*, 1974]. We have checked that changing the time steps does not affect the results that we will present, so that we have achieved a continuum in time. It is one of our purposes in this paper to demonstrate that our results also do not depend on the spatial resolution, so that we have achieved a continuum in space as well.

The numerical catalogue of events is generated is as follows. Starting from any initial condition where the displacement along the fault is nonuniform, the system self-organizes into a statistically steady state which is independent of the initial conditions. We begin collecting data after the self-organized state has been reached. The system is loaded continually at the slow loading rate. The fault remains locked while the stress at the fault boundary is less than the frictional strength. When the stress reaches the sticking friction, the fault begins to move. Because of the friction that we are using, for unstuck patches less than the critical stiffness length $\hat{x}$, the fault will slide stably (creep) at rates which scale with the slow loading rate. We therefore define an event as initiating when some part of the fault has a velocity that exceeds some multiple of the plate-loading rate, and an event as ending when all of the fault has a velocity that has then dropped below a multiple of the plate-loading rate for some amount of time. We typically use a multiple of 10 being the factor a_i for initiating an event, a multiple of 5 being the factor a_f for finishing an event, and a time 0.2 for the fault having remained below the $a_f\nu$ finishing velocity cut. We have checked that the results at large scales are not sensitive to the choice of these numbers; only at the nucleation scale, where there are creep surges which occur at many times the plate loading rate, is there any issue. Then a large value of the cutoff factor a_i is useful in removing them.

3.1. Bulk Dissipation

Because we have elastic radiation emitted during the events, and boundaries which reflect some of the radiation, we need to use some type of bulk dissipation to damp out the elastic waves in the bulk between events. We have examined a number of different ways of adding dissipation to the bulk, all of which give results that behave similarly. None of them match the form of dissipation which best describes the Earth [*Aki and Richards*, 1980; *Sipkin and Jordan*, 1979]. However, since the dissipation in the Earth is very weak at scales near the source, the bulk dissipation should not be an important effect on the source dynamics, and all of the forms of dissipation that we examine share that property. And again, all of them give the same results.

In one case, we add dissipation to the bulk in the form of a Kelvin-Voigt viscoelastic model (stress in bulk equals strain plus constant Γ times strain rate) with a coefficient that depends on the distance y from the fault; equation (1) becomes

$$\frac{\partial^2 U}{\partial t^2} = \nabla^2 U + \nabla \cdot \Gamma(y) \nabla \frac{\partial U}{\partial t} \quad . \tag{22}$$

In an alternative case, we used a bulk dissipation that ties the velocity to the reference tectonic velocity, so as to represent substrate drag, again with a y dependence:

$$\frac{\partial^2 U}{\partial t^2} = \nabla^2 U + \Gamma(y)(\nu - \frac{\partial U}{\partial t}) \quad . \tag{23}$$

In a third case, we studied a bulk dissipation which uses the elliptic boundary value problem to quench the internal kinetic waves. The procedure is as follows. Once the maximum velocity on the fault drops below the cutoff for ending an event, and does it for a sufficient amount of time, we check to see whether the static elastic solution for the current boundary displacement has all the stresses not exceeding the friction strength. This static solution is found by solving the Dirichlet boundary value problem for Laplace's equation (the static scalar elastic equation) with the stuck fault and loading surface as boundaries, and, as in the dynamics, peri-

odic boundary conditions along the fault. There are two possibilities. If the static solution has a stress at some point on the fault which exceeds the friction strength, then we know the event is not finished. Hence we resume the full elastodynamic simulation as before, continuing from where we had interrupted to do the check. If, instead, the static solution indeed has all parts of the fault below the sticking friction strength, then we consider the event done. We then replace the kinetic bulk with the static bulk elastic solution. The bulk velocities are also reset, by updating the boundary displacements which are creeping, displacing them for a small finite time, finding the static solution for this future time, and then setting bulk velocities to the difference between the two static solutions divided by the time increment. This sets all the velocities less than or equal to the creep speed. This method of dissipation was studied using the second algorithm, which solved for displacement and velocity, using fast elliptic solvers for displacements.

Again, all three methods of dissipating energy in the bulk give the same result. We used these different types of dissipation to show that the details of the loading process and the bulk dissipation are unimportant. They each have quite different dispersive properties for the waves impinging on the loading surface, and quite different time dependences of the dissipation and dispersion of different wavelengths. It is, in fact, quite interesting that the details of the bulk dissipation and dispersion have quite unimportant effects on the behavior; much more important, as we will see, is the friction on the fault.

3.2. Events

After an event is completed, we analyze the properties of the event that just occurred, and continue loading until the next event occurs, and the cycle is repeated. There are a number of properties of each event we can measure. The moment M measures the net slip in an event. To conserve moment, we measure the slip from the last time an event occurred there with that minimum velocity. Thus

$$M = \int \delta S(x) dx \,, \tag{24}$$

where $\delta S(x)$ is the net slip measured since the last net slip event occurred at the location x and is zero unless a velocity, taken to be $a_i \nu$, has been exceeded. The only issue in how exactly one defines the moment is how to consider creep displacements. However, since the seismic part of the slip dominates the sum, and the slow creep is basically negligible, it does not matter. The magnitude of an event is the logarithm of the moment: $\mu \equiv \log_{10} M$.

We measure the length of an event in two different ways. The length Δ measures all the parts of the fault that have slipped at a velocity which exceeded the cutoff minimum velocity needed to initiate an event. The slip zone size length L measures the size of the spatially connected fault patch which moved at all, at the place surrounding the location on the fault which slipped the fastest during the event. As we will see, this length L is particularly useful in examining nucleation questions.

3.3. Parameters

Before turning to the series of plots which form the core of our results, we discuss here the different parameters in the problem, their relevance, and the reasons we have chosen the ranges of values that we study. There are two main sets of parameters: one set describes the bulk, and the other describes the friction. A further distinction can be made between those parameters which turn out to be relevant, and those which turn out to be irrelevant to the resulting behavior. Even for those that do turn out to be relevant, we will see, quite fortunately, that for nearly all those parameters the behavior scales in a simple way with the parameter, in the regimes that will be of interest.

The bulk is described by the geometry and boundary conditions away from the fault. For a big enough and sufficiently resolved bulk, all of the bulk parameters are either irrelevant or unimportant. We consider a rectangular geometry of a plate of length L_x and width $L_y \equiv 1$. For long enough faults, L_x becomes an irrelevant parameter if the model does actually exhibit a broad distribution of rupture sizes, i.e., type (I) complexity. The longest events will then not break the whole fault length, and changes in L_x do not affect the statistics. For short enough faults, the longest events do break the whole length, and the longest events therefore scale with L_x. In that case, the statistics of the events do depend on L_x. We need to be concerned if the transition value of L_x is longer than for the major faults typically found in the Earth's lithosphere (often it is). *Horowitz and Ruina* [1989], in their quasi-static study that was stabilized by the onset of velocity strengthening at higher slip rates, noted the importance of L_x for complexity. They reported that complex solutions, with features roughly like what we have called large event complexity, type I, above (i.e., their Figure 10), had been found only at large values of L_x. They show such a case for $L_x = 20\pi \approx 63$, but show another (their Figure 9) with notably less complexity at that same L_x but larger critical stiffness of the fault law relative to the elastic unloading stiffness of the surroundings.

The resolution of the grid in the x direction is δx, and the resolution in the y direction is δy; we have refined the grid such that the results do not depend on these parameters, thus demonstrating a spatial continuum limit. We find that we need to make δy small enough compared to δx to get a convergent response; $\delta y / \delta x = 0.5$ is sufficient in the parameter ranges we study. We would, ideally, like to make the grid resolution extremely fine. This is, however, a very expensive limit, with the cost scaling as the cube of the degree of refinement (one degree each from the two spatial degrees of freedom, and a third from having to take smaller time steps to resolve the faster associated frequencies).

The other bulk parameters are associated with the wave dissipation $\Gamma(y)$. As the results do not depend on which type of dissipation we use, in the ranges we have used, these parameter values are not important. There are, nevertheless, values which give the most efficient damping. Since the quenched dissipation (third case, described after equation (23)) removed the bulk kinetic energy most rapidly, we

generally used that in the calculations of the nucleation processes. In the case where we used continuous dissipation, the viscous form (first case) was seen to dissipate kinetic energy the fastest, and was the preferred method. There, typically, we used a linear form of $\Gamma(y)$, with

$$\Gamma(y) = \begin{cases} 0 & y \le y_0; \\ a(y - y_0) & y > y_0 \ . \end{cases} \tag{25}$$

For $y_0 = 0.5$, the viscous dissipation (22) with a value of $a \approx 0.4$ was seen to dissipate the bulk kinetic energy most rapidly; however, this large value required a smaller time step, owing to the numerical stability conditions, so we generally compromised with a smaller value, a compromise being $a = 0.2$. Again, though, none of these choices were important to the results. It is one of the features of our findings that we wish to emphasize that the results that we present are insensitive to the bulk dissipation and dispersive properties.

The loading rate parameter ν sets the timescale between events, and sets the velocities in the creep regime, but is otherwise unimportant for the dynamic events. We want ν to be small so as to make this separation of relevance and irrelevance clear (and to match the extremely small values that occur in the Earth), but not so small that is takes too long to accumulate much loading. (*Rice and Ben-Zion* [1996] and *Lapusta and Rice* [1997] have developed a boundary integral model with a spectral formulation that allows for arbitrarily slow loading rates.)

There are five friction parameters in our model: α, β, σ, γ, and η. A sixth, the threshold value Φ_0, is irrelevant and can be scaled out of the problem; this follows from the linearity of the bulk equations, which allows the addition and subtraction of a constant stress solution,

$$\Phi \to \Phi - \Phi_0 \qquad U \to U + \Phi_0 y \ . \tag{26}$$

As a consequence, as in earthquakes, only stress drops, not absolute stresses, are relevant (in thermo-mechanically uncoupled models). We have already used a nondimensionalization to set the scale of the maximum friction drop from the large-scale α weakening in (7) to unity.

The parameter γ sets the timescale of the healing of the friction. When the time $1/\gamma$ is long compared to the rupture timescale, we get slip weakening. When $1/\gamma$ is short compared to the rupture timescale, we get velocity weakening [*Shaw*, 1995]. Since we want healing between events, we need

$$\nu \ll \gamma \ . \tag{27}$$

In the slip-weakening case, when $\gamma \ll 1$, γ is seen to be an irrelevant parameter.

The parameter η, which controls the viscous strengthening, is included to give stability to the smallest wavelengths (see (16)-(18)). It does not affect the behavior qualitatively when it is small.

For the case of laws with a single weakening process, that leaves a single relevant parameter. We may describe that scale, equivalently, for slip weakening by either saying that (1) $\alpha = 0$, σ is irrelevant beyond providing the scale of the strength drop (it could be rescaled to unity) and the parameter is β, or (2) $\sigma = 0$, β is then without effect and the parameter is α. This one-process case can be treated as a special case of what follows.

For laws with a pair of weakening processes, that leaves us with three relevant parameters: α, β, and σ. The parameter σ sets the scale of the stress drops of the small events. Stress drops of earthquakes are observed to be roughly equal for small and large events, so this suggests a value of σ closer to unity would be the more realistic value. Alternatively, we could accept arbitrarily small values of σ, provided that α was made large (so that $\pi/\alpha \ll 1$, in the slip-weakening case); if we then assume that observable earthquakes only occupy the length scale range larger than π/α, the invariance of stress drops for observable events would be respected in this slip-weakening case. However, this regime is difficult to resolve numerically.

The parameter β sets the scale of the smallest events in the two-process case. For slip weakening, the nucleation length, from equation (14), is $\pi/(\beta + \alpha)$, while for velocity weakening, from equation (18), it is $\pi\sqrt{\gamma\eta/(\beta + \alpha)}$. We would like to have this length be very small and, also, to have the initial drop in friction happen rapidly compared to any overall weakening effects; thus $\beta \gg \alpha$ is the desired regime. In practice, however, if we want to resolve the nucleation length with the grid resolution, we cannot use such large values of β. Nevertheless, we will see that we obtain appropriate scaling with the range of β that we can achieve.

The crucial parameter in the problem is α in the case of slip weakening, and α/γ in the case of velocity weakening. This sets the behavior of the large events (or of all events in the one-process case), and rates of small events when there are two processes. It both qualitatively and quantitatively changes the behavior in the model. It needs to be larger than unity in order to make the large-scale weakening unstable in the problem. The most realistic range of stress drop invariance occurs when σ is order unity or when σ is small but α is very large, as above. However, the special parameter range allowing full small- and large-event complexity in this two-dimensional uniform fault model is with small σ and α near 3. Then there are numerous small events. For larger values of α we get few small events.

Even with our relatively modest parameterization, we would still have a huge space to check if we were to try to check all of parameter space. Instead, we will focus on first showing results for a range of parameters which illustrate the conclusions that we have already announced, discussing these results within the emerging theoretical insights developed from this and earlier studies. Because of the theoretical interest in the special parameter range for which small-event complexity results, we devote a series of figures to that case.

For the bulk, we use $\nu = 0.0001$. In general, we use $L_x = 200$, $\delta_x = 0.1$ and $\delta_y = 0.05$, although further refinement is sometimes necessary. The special parameter range which has shown small-event complexity is, for the slip-weakening case, $\alpha = 3$ (which means that what would reduce to a nucleation size π/α in the limit $\sigma = 0$ is then tuned to unity), small σ of order 0.1 or less, and β much larger than α. For exam-

ple, $\alpha = 3$, $\beta = 9$, and $\sigma = 0.03$ are used in several figures here to illustrate that parameter range. When such cases are studied with higher resolution, we use $L_x = 100$, $\delta_x = 0.05$, and $\delta_y = 0.025$.

4. Results

4.1. Single Weakening Mechanism

We consider first the case of a singe weakening mechanism, $\sigma = 0$ (so that β is irrelevant). We then will wish to choose the nucleation size π/α much smaller than crustal dimensions. There is a well-established framework for anticipating some features of the event population. We expect slip to begin aseismically when the highest-stressed position on the fault just reaches the threshold stress. Then the aseismically slipping zone will gradually enlarge in size until it has reached a spatial extent comparable to what is called the nucleation size, and is denoted by $\hat{x}$ ($\approx \pi/\alpha$, for $\alpha \gg 1$, for the present laws). At that point, rapid slip breaks out as a propagating rupture. This scenario is supported by all known elastodynamic simulations of earthquake sequences that fully model nucleation [*Rice and Ben-Zion*, 1996; *Ben-Zion and Rice*, 1997; *Lapusta and Rice*, 1997, 1998], and was already apparent in earlier works that did not do full elastodynamics [*Tse and Rice*, 1986; *Rice*, 1993]; it is supported by our present studies. Once dynamic rupture breaks out, with the single weakening mechanism it will generally occupy a region much larger than the nucleation size. In some cases, that region occupies the entire fault domain, whereas in others a population of large event sizes develops. As anticipated from *Horowitz and Ruina* [1989] and *Carlson et al.* [1991], we find for the present cases that sufficiently large L_x always leads to a broad population of (large) event sizes. The smaller the nucleation size, the larger the L_x value required [*Shaw*, 1995]. It may be long compared to natural examples.

For example, Figure 1 shows two different representations of the slip history produced by the model when $\alpha = 16$. In this case the nucleation size is $\pi/16 = 0.20$. In general, only large events are seen. Only part of the long space and time history is shown (the fault length, in this case, is twice what is shown). Faintly visible, in the upper Figure 1a, are what look like some exceptions to this. They consist of two types of motions. First, there are isolated patches which can be triggered by dynamic waves from an event. When we count events numerically with our event-counting criteria, these multiple patch events are considered as one event, and small isolated patches triggered by dynamic waves from larger events do not end up being counted as separate events. There is a second set of motions, rarer than any of the others, which occasionally show up, and are due to finite resolution. Near the nucleation scale, there may be the occasional creep surge in these plots. Slower loading and a more resolved grid remove even these last vestiges of creep surges. However, these limits are very costly to implement for such long loading, and we therefore tolerate these extremely rare exceptions here. Higher cutoff velocities can also remove them; we do not, however, want to eliminate small events simply by virtue of having set the cutoff velocity too high.

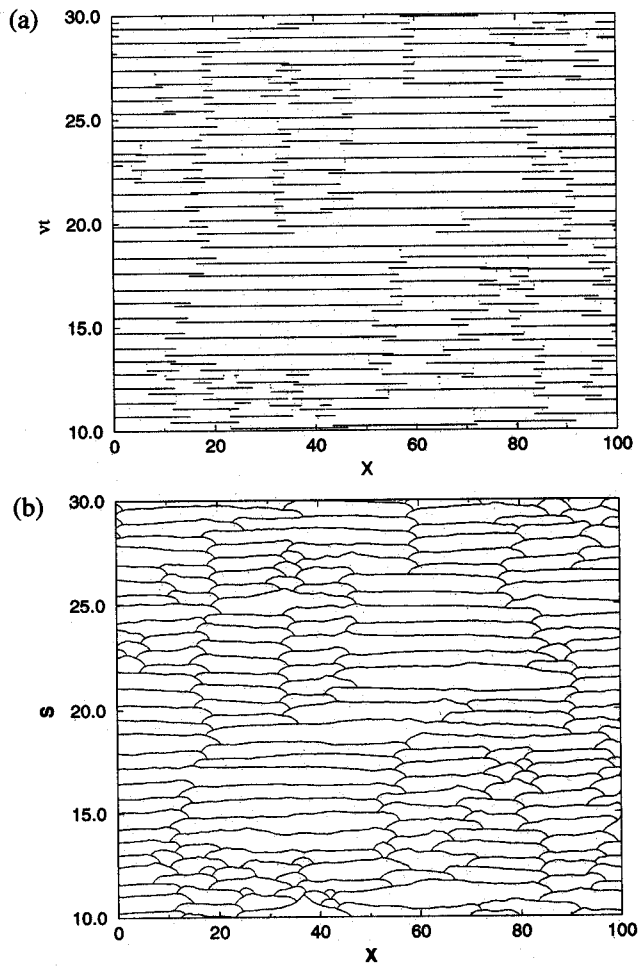

Figure 1. Two different representations of an attractor produced by the model for a single weakening mechanism. The horizontal axis is distance along the fault, measured in units of the brittle crust depth. The material properties are uniform along the fault. (a) The times at which various parts of the fault break– a standard space-time plot in seismology, only here for very many loading cycles, whereas only a fraction of a loading cycle is generally available for real data. (b) The cumulative slip along the fault following an event, for the same set of events as above in Figure 1a. The friction parameters used here are $\alpha = 16$, $\sigma = 0$, $\gamma = 0.1$, and $\eta = 0.00001$

These rare surges are restricted to being close to the nucleation length scale; they are, however, occasionally counted as events by the picking criteria we use. They differ in two significant ways from the small events that we will see when we consider two weakening mechanisms. First, they are not broadly distributed over a range of length scales, but rather peak about the nucleation scale. Second, and most significantly, these surges exhibit sensitivity to the grid resolution, with their rate of occurrence changing markedly as the grid becomes more resolved. This is in stark contrast to the small events that we will see when we introduce two weakening mechanisms, which are insensitive to grid resolution. A related symptom of the grid resolution problem for the surges is the nonmonotonic parameter dependence in the surge rates;

as we change α, we change the nucleation length scale $\hat{x}$, and as this becomes a favored and disfavored multiple of the grid resolution, we get nonmonotonic changes in the number of surges as a function of α at fixed grid resolution. This is again in stark contrast with the small events that we will see when we introduce two weakening mechanisms, where we see steady changes in the distributions of events as the parameter values are changed. Aside from these rare nucleation scale surges, essentially all of the events have lengths much larger than the nucleation size, and, indeed, for large α, it is rare to see events with lengths smaller than about 4 to 6 (i.e. 4 to 6 times seismogenic thickness), which is, for this value of α, 20 to 30 times the nucleation size and would correspond to lengths like 40 to 90 km for strike-slip faults with 10 to 15 km seismogenic depth. Hence the model suggests that essentially all events will be large events in the case shown. The events do not repeat periodically in the long term, although there are many locations at which sequences of, say, four to eight very similar events occur with roughly uniform recurrence intervals.

There is a distribution of large event sizes, although we emphasize that this occurs only because the modeled region is sufficiently long. For the case shown, that length is 200, which means 2000 to 3000 km for strike-slip faults in nature, comparable to the entire length of the San Andreas or North Anatolian systems. If we had modeled a region of, say, 25 length (250 to 400 km in nature, already rather long for strike-slip faults), the simulations would not give large-event complexity but, rather, a nearly periodic sequence of large events that rupture the entire region.

What happens as we vary α (and hence the nucleation size $\pi/\sqrt{\alpha^2 - 1}$, which, from here on, we will approximate by π/α)? Figure 2 shows size distributions for a range of α. As long as the nucleation size is small compared to unity, i.e., to seismogenic thickness, the slip history is similar to that shown. There are no small events, and the larger the α, hence the smaller the nucleation size π/α, the larger the minimum size of those large events and the longer the length needed to give a broad size distribution (versus nearly periodically repeated events that span the domain). However, a transition occurs if we diminish α so much that the nucleation size becomes comparable to the seismogenic thickness. The minimum event length of the population tends to approach the seismogenic thickness and a broader distribution of events, bordering on the nucleation size, then emerges.

For example, we see in Figure 2 that the large-event peak extends down to near 5 when $\alpha = 16$ ($\pi/\alpha = 0.20$) and down to near 4 when $\alpha = 8$ ($\pi/\alpha = 0.39$). However, in the cases $\alpha = 6$ ($\pi/\alpha = 0.52$) and $\alpha = 4$ ($\pi/\alpha = 0.78$), the peaks extend down to near 2. These lower peak events of the large-event population finally merge with the nucleation length around $\alpha = 3$ ($\pi/\alpha = 1.1$). That is not a physically interesting range of α for a model with a singe weakening mechanism since it precludes all earthquake nucleation with length smaller than seismogenic thickness. However, we will see that the choice of α in this special range, around 3, in models with a pair of weakening mechanisms, is part of the special parameter range leading to small-event complexity (the other part being a small strength drop σ in the first, small-slip, weakening process).

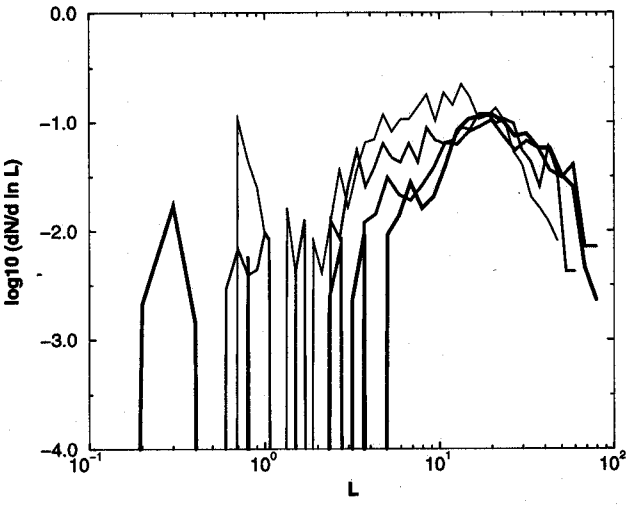

Figure 2. The distribution of lengths L of events for the slip-weakening friction with different α for the case when $\sigma = 0$. The differential number of events in a logarithmic interval of lengths is plotted against the event length. Note that we now have essentially only large events, aside from a few fluctuations near the nucleation scale. Four values of α are used here, $\alpha = 4$, 6, 8, and 14. Increasing line thickness corresponds to increasing values of α.

Our results with small nucleation sizes in this case of a single weakening mechanism are consistent with the results of *Rice and Ben-Zion* [1996] on continuum fault models, that dynamic events burst from the nucleation size to a much larger size, and that there are no small events, and hence no small-event complexity.

4.2. Pair of Weakening Mechanisms

Now consider a nonzero σ and associated parameter β. Under continuous loading, slip initiates when the highest stress just reaches the threshold stress and continues aseismically until the sliding region occupies an extent comparable to the nucleation size $\hat{x} = \pi/(\alpha + \beta)$, at which point a dynamic breakout occurs. However, in this dynamic breakout, the stress drop near the nucleation site is just of order σ, at least before enough slip takes place so that the large-scale weakening process is activated (it could cause a further drop of 1, for a total stress drop of $1 + \sigma$ in these frictions with two weakening processes). Now suppose that σ is extremely small, yet still positive, and that the stress field at the moment of nucleation is spatially heterogeneous. In such a case, there arises the possibility that the rupture will propagate into a region where the initial stress was more than σ away from threshold. Then, for small slip such that the large-scale weakening process does not contribute significantly, this generates a region of negative stress drop that will arrest the rupture. These considerations lead us to suspect that the introduction of sufficiently small $\sigma > 0$ will always lead to some distribution of small events, at least when the stress field stays spatially heterogeneous from event to event.

If the nucleation size that would result when $\sigma = 0$, namely, π/α, is much less than unity, then we expect that the ruptures of such small-event distribution might not stop once they reach size π/α, so that instability based on the large-scale weakening process sets in. Thus we then expect the small-event population to mainly occupy only the size range between $\pi/(\alpha+\beta)$ and π/α.

We have no complete theoretical explanation of this regime, but simulations do indeed show that when that nucleation size $\hat{x} = \pi/\sqrt{\alpha^2-1}$ is comparable to or a little larger than unity we can retain enough heterogeneity of stress in the system to allow that event population, associated with initially small strength drop $\sigma > 0$, to span a range of sizes, from $\pi/(\alpha+\beta)$ to sizes even larger than $\pi/\sqrt{\alpha^2-1}$. In particular, we find in simulations that if $\alpha = 3$ (so that $\hat{x}_{\sigma=0} \approx 1.1$), if $\beta \gg \alpha$ (e.g., $\beta = 9$ or larger) and if σ is small (e.g., $0 \leq \sigma \lesssim 0.1$), then there is a small-event distribution of power law frequency-size statistics, which results as a legitimate outcome of a continuum model. Fortuitously, *Myers et al.* [1996] focused in their simulations on precisely this parameter range, leading them to suspect that they were seeing a universal feature of dynamic fault models. We establish in the present work that such a power law distribution truly exists, but also show that it does so only in that special parameter range, and that, consistent with the above discussion, it does not exist when either σ is large, of order 1, or when $\alpha \gg 3$, so that $\hat{x}_{\sigma=0} \ll 1$.

In fact, *Ben-Zion and Rice* [1997] had already forecast what we find here, namely, that the tuning of the nucleation parameter $\hat{x}_{\sigma=0}$ to crustal dimensions was important in obtaining the power law small-event range of *Myers et al.* [1996] and *Langer et al.* [1996], although they also raised

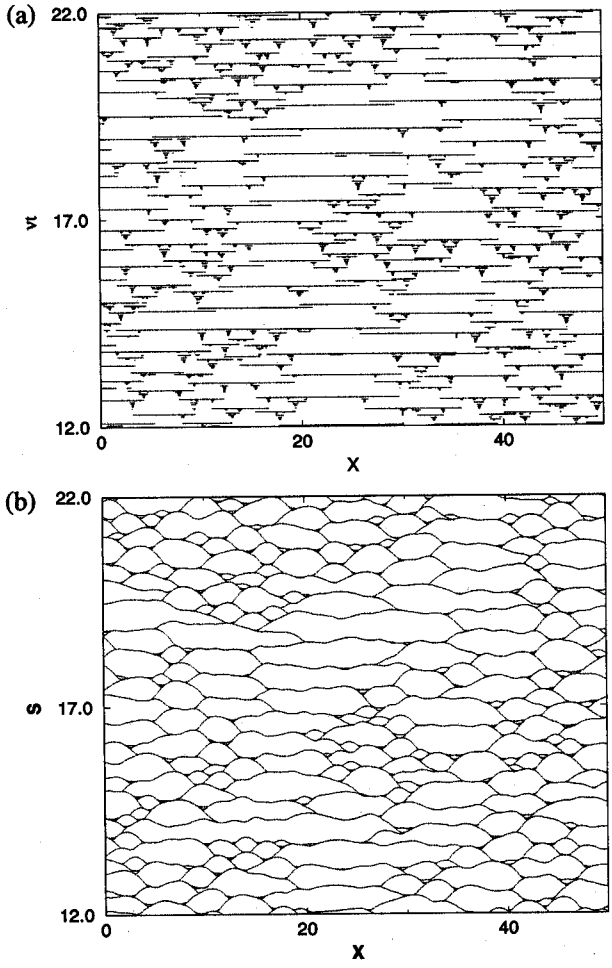

Figure 3. Two different representations of an attractor produced by the model for the special parameter range where numerous small events exist. The special parameter range consists of two weakening mechanisms with α close to 3 and σ small. The same type of plots as in Figure 1 are shown, but with the axes rescaled somewhat. (a) The times at which various parts of the fault break. (b) The cumulative slip along the fault following an event, for the same set of events as in Figure 3a. The same set of parameters as in Figure 1 is used, except now $\alpha = 3$ $\sigma = 0.03$, and $\beta = 13$. Note the rich population of smaller events, for this friction.

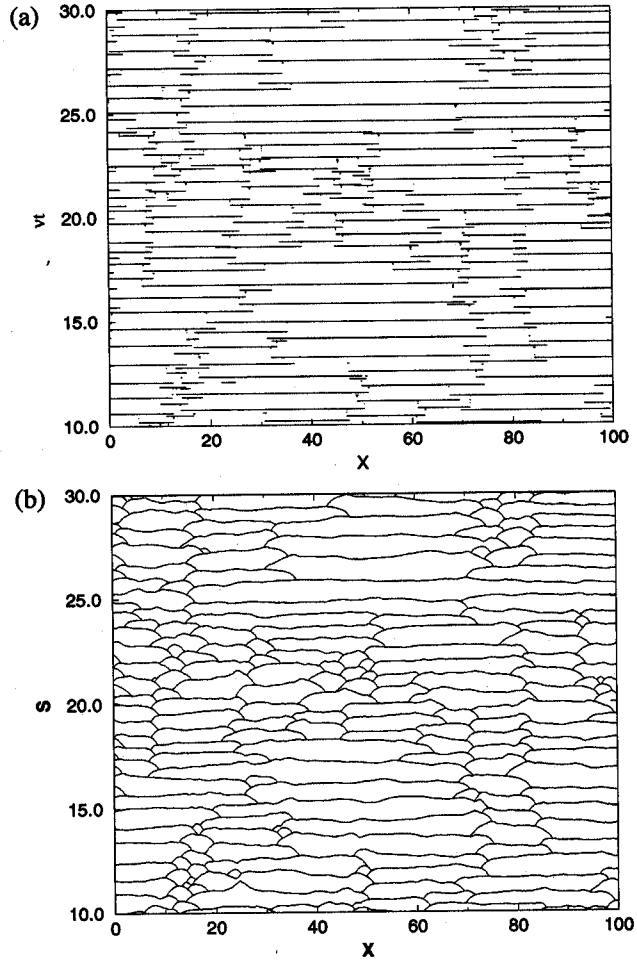

Figure 4. Two different representations of an attractor produced by the model where two weakening processes are used, with the small-scale nucleation size being the same as in Figures 1 and 3, but now with α significantly larger than the critical value. (a) The times at which various parts of the fault break. (b) The cumulative slip along the fault following an event, for the same set of events as in Figure 4a. The same set of parameters as in Figure 1 are used, except now $\alpha = 8$, $\sigma = 0.03$, and $\beta = 8$.

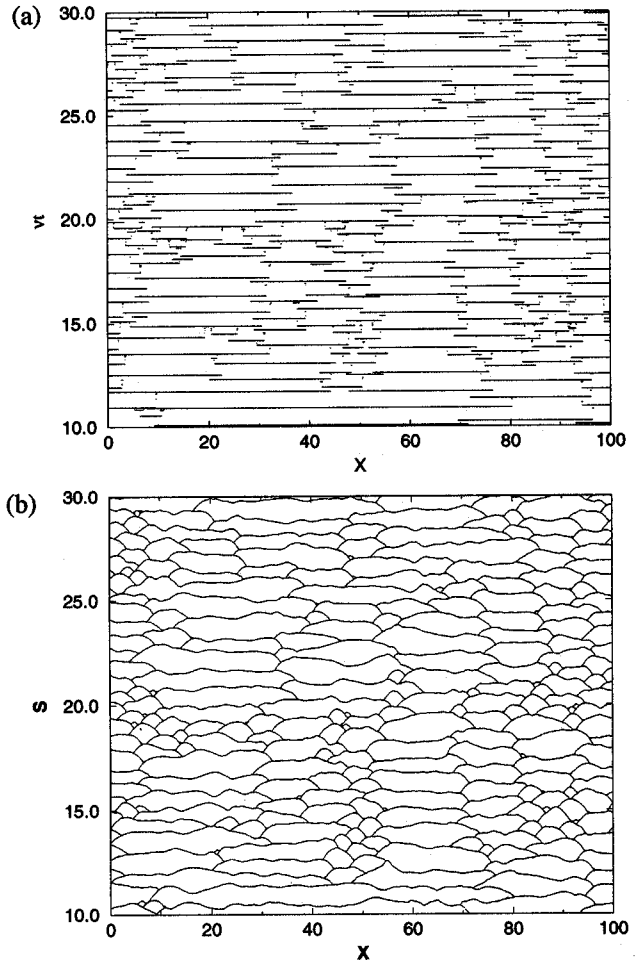

Figure 5. Two different representations of an attractor produced by the model where two weakening processes are used, but σ is large. (a) The times at which various parts of the fault break. (b) The cumulative slip along the fault following an event, for the same set of events as in Figure 5a. The same set of parameters as in Figure 1 are used, except now $\alpha = 3$, $\sigma = 0.3$, and $\beta = 13$.

the question of if the simplified time-dependent strength drop σ of those studies had rendered the system inherently discrete. We now find that this latter question is not the issue; rigorous modeling of the small-scale weakening process still produces power law small-event complexity so long as α is near 3 ($\hat{x}_{\sigma=0}$ is near 1) and σ is small.

As an example, we show in Figure 3 the two representations of the slip history when $\alpha = 3$, $\beta = 13$ and $\sigma = 0.03$. This has the same nucleation size, $\pi/(\alpha + \beta) = 0.20$, as does the case in Figure 1, but even casual inspection shows that something remarkably different is going on. There is a broad distribution of sizes, with many small events. Further, as we analyze in detail in a subsequent sequence of figures, the small-event population forms a power law distribution.

To emphasize, however, that this remarkable behavior occurs only in a very special parameter range, and not for all models with a pair of weakening mechanisms, we show the following examples of event distributions: Figure 4, for $\alpha = 8$, $\beta = 8$, and $\sigma = 0.03$, and Figure 5 for $\alpha = 3$, $\beta = 9$, and $\sigma = 0.3$. These are both substantially depleted of small events, compared to Figure 3, and are, visually, much like Figure 1. These cases emphasize that when the model incorporates only one of either small σ (Figure 4) or $\alpha \approx 3$ (Figure 5), the results are significantly different from the special case (Figure 3). We cannot illustrate the entire parameter range, but when α is much larger than 3, and when σ is much larger than, say, 0.05, the results are much more similar, visually, to Figure 1 ($\alpha = 16, \sigma = 0$) than to Figure 3 ($\alpha = 3, \sigma = 0.03$). For example, Figure 6 shows results for $\alpha = 8$, $\beta = 8$, and $\sigma = 0.3$; the results are qualitatively quite similar to those of Figure 1.

4.3. Special Case with $\alpha \approx 3$ and σ Small, and Variations

Because of the theoretical interest of the small-event complexity in the special case $\alpha \approx 3$, β much larger, and σ small, we now focus on that case and the effect of parameter varia-

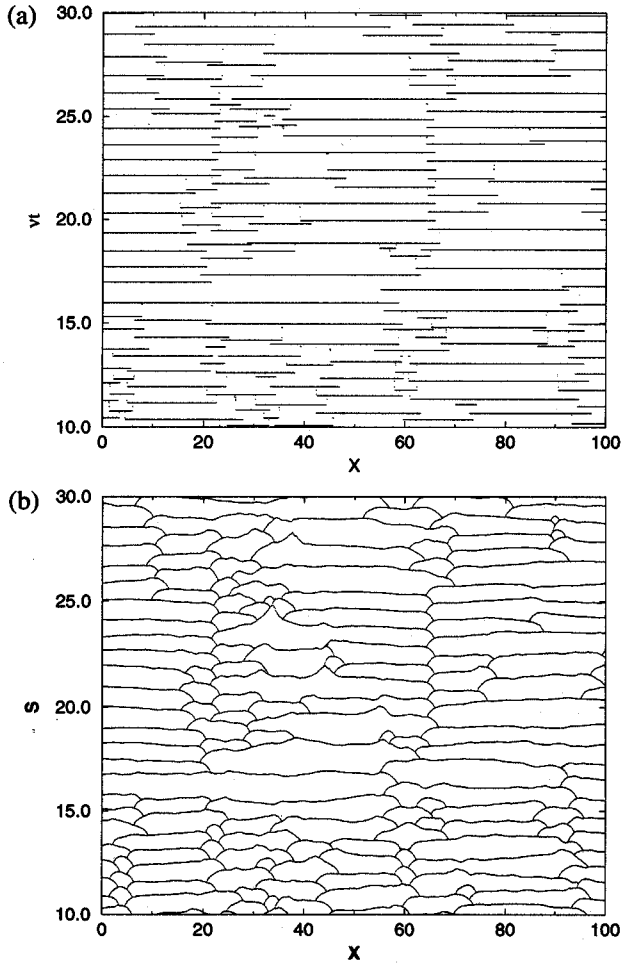

Figure 6. Two different representations of an attractor produced by the model where both α and σ are large. (a) The times at which various parts of the fault break. (b) The cumulative slip along the fault following an event, for the same set of events as in Figure 6a. The same set of parameters as in Figure 1 are used, except now $\alpha = 8$, $\sigma = 0.3$, and $\beta = 8$.

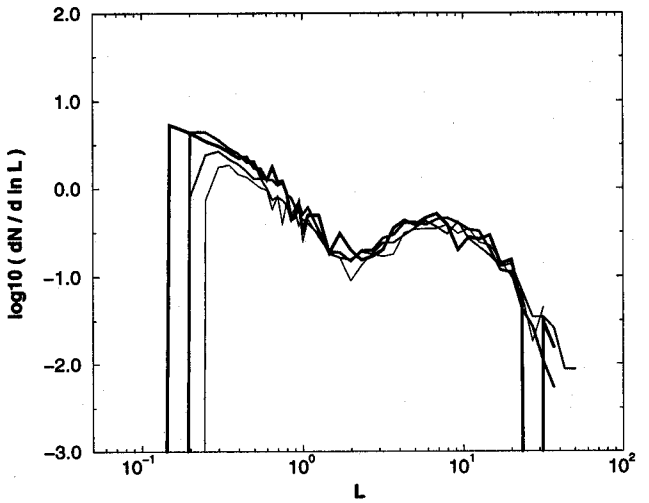

Figure 7. The distribution of lengths L of events for different slip weakening lengths $1/\beta$. Four values of β are used, $\beta = 9$, 12, 15, and 21. Increasing line thickness corresponds to increasing values of β. Note the shift of the cutoff small-event peak to smaller lengths $\hat{x}$ for larger values of β, as expected. The nucleation scale lengths for these four values of β for the large scale weakening $\alpha = 3$ used here are, respectively, 0.262, 0.209, 0.175 and 0.131, for increasing β. Note the good quantitative correspondence with the smallest event length cutoff. The grid resolution here is $\delta_x = 0.05$, while $\sigma = 0.03$.

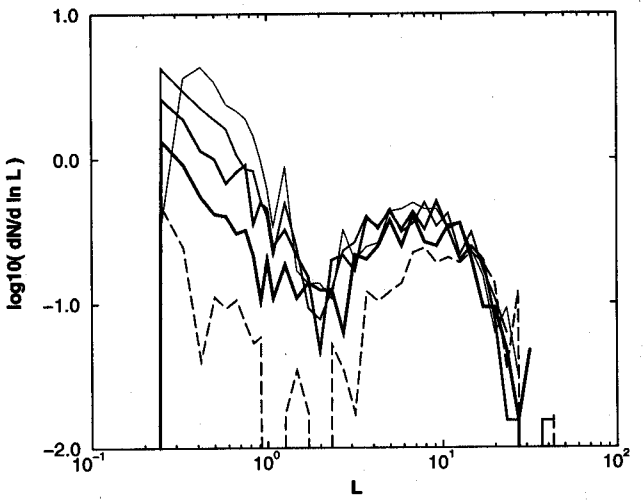

Figure 8. The distribution of lengths of events for different small event stress drops σ. Five values of σ are used, $\sigma =$ 0.01, 0.02, 0.04, 0.08 and 0.2 . Increasing line thickness corresponds to increasing values of σ, except for the dashed line which has $\sigma = 0.2$. Note the decreased number of small events for larger values of σ. The weakening parameters are $\alpha = 3$ and $\beta = 9$.

tions within it and from it. We will look at distributions of lengths, rather than distributions of moments, as it is easiest to make direct quantitative comparisons with nucleation length scales associated with slip-weakening lengths. Plots of the corresponding distributions of moments further reinforce the results we describe, and only illustrate more clearly the existence of power law distributions.

First, we show in Figure 7 the event rates versus rupture length for $\alpha = 3$, $\sigma = 0.03$, and a broad range of β values, $\beta = 9$, 12, 15, and 21. We see that results basically fall on top of one another, except for the population suddenly dropping to zero at a size around the theoretical nucleation size $\pi/(\alpha + \beta)$, which then ranges from 0.262 when $\beta = 9$ to 0.131 when $\beta = 21$.

Figure 8, for $\alpha = 3$ and $\beta = 9$, shows how the event frequency versus rupture length is affected by varying σ. We see results for small σ values in Figure 8. For $\sigma = 0.01$ to 0.08 the event frequencies are broadly comparable and are compatible with the power law distribution. However, the results for larger values of σ show very clearly that there is a diminished number of small events, and a significant change in the distribution as σ becomes (moderately) large.

Finally, we show the effect of change of α away from its special value, when σ is small. Thus Figure 9 shows the event frequency versus rupture length for $\sigma = 0.03$, $\beta = 9$, and for a range of moderate α values, $\alpha = 3$, 4, 6, and 8. The results show clearly that detuning α from 3 severely depletes the small-event distribution. The α dependence for the larger events is broadly similar to that shown in Figure 2 for the $\sigma = 0$ case (i.e., for a single weakening mechanism).

4.4. Some Generalizations

Having studied one case in detail, we would like to know how these results generalize. Here, we briefly comment on the results of changing three different features: changing the nucleation mechanism, changing the frictional instability, and changing the bulk dispersive properties. In each of

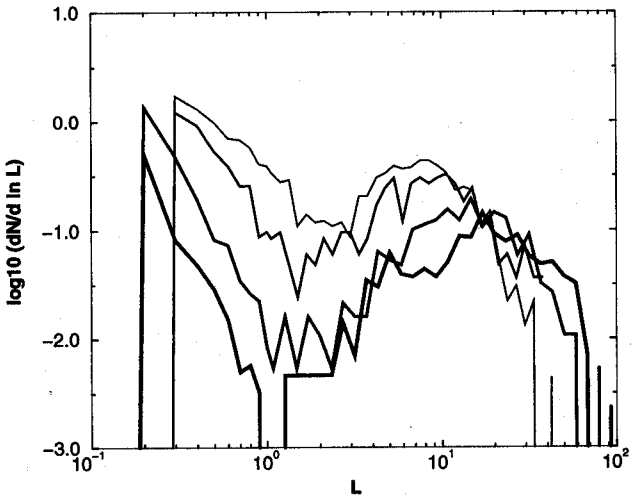

Figure 9. The distribution of lengths of events for different α. Note that both the large- and small-event rates are affected by α. Four values of α are used here, $\alpha = 3$, 4, 6, and 8, with the larger values of α having the biggest large events. Increasing line thickness corresponds to increasing values of α. Note the shift of the peak of small events toward smaller values of L for larger values of α. The nucleation lengths $\hat{x}$ are, respectively, 0.262, 0.242, 0.209, and 0.185 for increasing α. The grid resolution here is $\delta_x = 0.1$; this coarseness is evident in the jump in the minimum length events between $\alpha = 4$ and $\alpha = 6$.

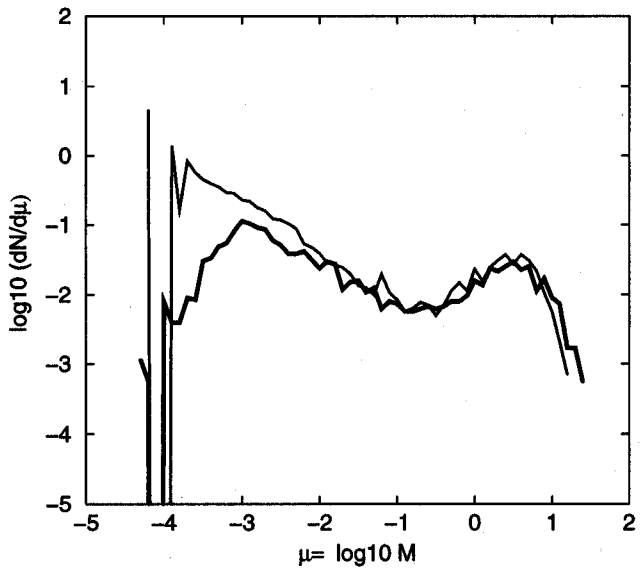

Figure 10. The distribution of sizes of events for two different nucleation mechanisms. The differential number of events in a logarithmic interval of moments is plotted against the magnitude (the logarithm of the moment). The frictions differ in the nucleation mechanism, but are otherwise the same. A slip-weakening nucleation mechanism and a time-dependent nucleation mechanism are shown. Both distributions have the same values of the overall weakening α and the small-event stress drop σ, but differ in the way that σ occurs. Aside from the smallest creeping scale, note that the two curves nearly overlay, showing the independence of the distribution of sizes at the large scales on the details of the nucleation mechanism, and the finite loading rate in one case. The thicker line is the slip-weakening nucleation, while the thinner line is the time-dependent nucleation.

these cases, we find results similar to what was discussed previously: a broad population of large events, and a population of numerous small events only in a special parameter range.

4.4.1. Nucleation mechanism. Changing from a slip-weakening nucleation to a time-dependent nucleation does not appear to change the results qualitatively. Near the critical parameter values, the distribution of sizes of events even quantitatively agree. Figure 10 illustrates this, plotting the distribution of length of events for two very different types of nucleation: one with the nucleation mechanism discussed in this paper where the stress drop σ occurs with a β slip weakening mechanism, and the other where the stress drop σ occurs in a time-dependent way, as in *Myers et al.* [1996] and *Shaw* [1997]. Other than the nucleation mechanism, all other parameters are the same. Observe that for events above the nucleation scale, for both the small and large events, the two curves are essentially identical. This plot was made for the large-scale weakening near the critical value; for values farther away the curves remain qualitatively similar, but begin to slightly differ quantitatively.

4.4.2. Velocity weakening. We can explore different frictional instabilities by changing γ in equation (8), going from slip weakening at small γ to velocity weakening at large γ, with a mixture in between. Our results are again similar to the slip-weakening case. In general, there is a broad distribution of large-event sizes. Only for small σ and for α/γ near a critical value do we see numerous small events. The critical value of α/γ is again around 3, with a minimum value of unity for getting the basic instability. This minimum value occurs when the frictional fault stress weakens at a rate equal to the natural velocity scale in the problem, which is the inverse radiation damping velocity, a velocity which is set by the shear wave speed multiplied by the strength drop divided by the shear modulus (all unity in our dimensionless variables, and thus corresponding to a radiation damping velocity of unity). This threshold value of unity for the dimensionless velocity weakening corresponds with an analogous critical velocity found by *Cochard and Madariaga* [1996], who saw small events in their model only when they tuned their velocity-weakening parameters to be close to the radiation damping velocity scale.

4.4.3. Bulk dispersion. The insensitivity of the results with respect to a number of aspects of the dispersion relation in the bulk is a feature of the behavior worth remarking on. *Shaw* [1997] showed that with the same friction, the distribution of sizes of events for the Klein-Gordon model (equations (11) and (2) [*Myers, et al,* 1996]) and the wave equation model (equations (1)-(3) [*Shaw*, 1997]) were nearly the same. These models have quite different dispersive properties at long wavelengths. Here we amplify this result, reporting that by using different $\Gamma(y)$ we again obtain essentially the same distributions for a given friction. Using a viscous dissipation, equation (22), and changing Γ, we change most strongly the dispersion of the small wavelengths. Taken together with changes in the degree of spatial regularization, we have a good exploration of the relevance of small-wavelength bulk dispersion to the results. Using the parameterization of Γ given by (25), we have examined distributions of sizes of events over a range of values of a and y_0, and gotten essentially the same results. Thus the results have been seen to be remarkably insensitive to both the long and short wave dispersive properties. This is very encouraging news for finite difference approximations, where dispersion is an intrinsic problem at underresolved wavelengths [*Alford et al.*, 1974]. It suggests much more robust results may be obtained than might have been thought. It also addresses a very important question about how much we need to know about the setting where earthquakes occur to get it right. Here we have seen that the results are sensitive to the fault properties. In contrast, the motions on the fault appear to be very much less sensitive to a number of aspects of the bulk properties

5. Conclusion

Our main conclusions have already been summarized in the abstract. Our results suggest that nonperiodic irregular large events are generic, in the sense that this occurs over a large measure of parameter space, in fault models that are sufficiently long compared to the seismogenic depth. The existence of numerous small events with a power law distribution of sizes, in contrast, appears to occur near a critical value, rather than above a critical value, and thus occurs over

a small measure of parameter space– at least in these two-dimensional models.

We have explained the existence of small events when there are two weakening scales and σ is small. In the limit as $\sigma \to 0$, these events would appear more like creep events, relative to the large weakening scale. Small events are possible because of sharply peaked stress concentrations which are left over by large events. The main question in obtaining small events is how large are the fluctuations left by the large events and how powerful are the small events in breaking through the more stuck neighboring regions. Increasing σ and α both contribute to the ability of small events to propagate, and increasing either was seen to lead to fewer small events, or to a complete absence of small events.

Despite the small parameter range over which somewhat realistic distributions of sizes of events occur, the mere existence of a spectrum of event sizes can be quite useful. Going beyond the question of what the distribution of sizes of events is, we can ask what the events themselves look like. So, for example, recent work has studied what the radiation from events for different sizes and different frictional instabilities looks like, finding, in particular, sensitivity to the source physics in the far-field radiated energy [*Shaw*, 1998].

What does all this mean for our understanding of earthquakes? The basic question underlying these investigations is the degree to which stress heterogeneities left by previous ruptures may be contributing to the complexity seen in earthquakes. Material and geometric heterogeneities also, no doubt, contribute to earthquake complexity. The question is, however, how much the dynamics may be contributing, and what the signatures of this contribution might be. There are a number of points to be made regarding this issue. First, this work has reaffirmed the existence of a profoundly complex attractor of the uniform dynamics in a region of parameter space. An impressive array of earthquake-like properties are exhibited in this regime. However, the region of parameter space over which one gets numerous small events with a power law distribution of sizes is very limited, at least in these two-dimensional models. Further, the small-event distribution changes continuously across this region, so there does not appear to be a special exponent of the power law. At the same time, these observations, though restricted in frictional parameter space, seem quite generic in other ways, transcending a variety of geometries, bulk dispersive properties, and types of frictional instabilities. So, what about earthquakes? Choosing an optimal parameter, the models show an astonishing array of earthquake-like behaviors. Earthquakes would, however, somehow need to organize their rupture process in order to operate in any particular parameter regime; and what might drive them to operate in any particular regime remains an open question. This situation raises a number of avenues of questions from the point of view of research. How well do the best regimes correspond with earthquakes? What might be added to make the best regimes correspond even better? What might be driving earthquakes to operate in those regimes? Might three dimensions be different?

We have shown that we obtain slip complexity under the most stringent conditions in a continuum setting. Further, we have seen that the complexity obtained is similar to that obtained when certain simplifications of the nucleation process are made. This provides convincing evidence that previous results with this class of constitutive laws describing elastodynamic slip complexity in homogeneous systems were indeed arising from a genuine continuum dynamical instability, and not because of numerical discreteness or algorithmic effects. It also suggests that further physics may be needed, however, if this special frictional parameter regime is to be broadened enough to have a chance of holding for earthquake faults. These results support the continued examination of slip complexity in uniform elastodynamic systems, and the extension to more realistic tensor, three-dimensional, as well as nonuniform elastodynamic systems. Most importantly, it challenges us to search for a correspondence between the complex behavior displayed by these models and the complex behavior displayed by earthquakes.

Appendix A: Dimensional Variables

In the body of the paper we have used dimensionless variable throughout. This has the advantages of preserving generality, identifying the relevant groupings of parameters, and presenting a minimal parameterization. To compare with observations, however, it is useful to go back and forth between dimensionless and dimensional variables, and so in this Appendix we list the conversions for a typical crustal case.

From the elastodynamic equation, the wave equation (1) in our scalar case here, we have three independent variables which can be scaled: space, time, and displacement. We scale space by the macroscopic geometrical lengthscale in the problem, the brittle crust depth W. This has a lengthscale of around 15 km in strike-slip environments, and a downdip length of around 60 km in subduction zones. Thus

$$x' = Wx\,, \tag{A1}$$

where the prime denotes the dimensional variable, and the unprimed is our dimensionless variable used in the body of the paper.

We set the dimensionless wavespeed to unity, which then sets the timescale as the time for a wave to travel W at the wavespeed c. Thus

$$t' = \frac{W}{c}t\,, \tag{A2}$$

For shear wavespeeds of 3 km/sec this gives a timescale around 5 sec in the strike-slip case, and around 20 sec in the subduction thrust case.

The last scaling comes from the displacements, where we have scaled the strength drop $\Delta\Phi$ of $1+\sigma$ to a strain $\Delta U/W$ of unity. Converting back to dimensional variables, using equation (2), we see

$$U' = W\frac{\Delta\Phi}{G(1+\sigma)}U\,, \tag{A3}$$

where G is the shear modulus of the material, and on the

fault U' corresponds to slip S'. Here $\Delta\Phi$ is the total strength drop, from the peak strength at onset of slip to the residual strength that is approached at sufficiently large and/or rapid slip; $\Delta\Phi$ includes the strength drops in both of the weakening processes we consider, hence the $1 + \sigma$, where the 1 corresponds to just the large scale weakening process.

If strength drop in the large scale process is comparable to the largest seismic stress drops in significant earthquakes, of order 10 MPa, and if $G = 30$ GPa, that corresponds to strain changes of order $3 \cdot 10^{-4}$ and displacements of order $3 \cdot 10^{-4}W$, which is about 5 meters in strike-slip environments. Such a 10 MPa total strength drop would generally be interpreted as implying that the peak strength is very low compared to an expected 100 MPa nominal rock friction strength because major faults consist of anomalously weak materials or are at high pore pressures. Alternatively, the 10 MPa strength drop could be consistent with the possibility that faults are strong, of the order 100 MPa peak strength, but that some as yet undiscovered mechanism could allow large slips at stresses comparable to that peak strength without significant weakening in the presence of the massive temperature rises thus implied.

One may instead argue plausibly that the peak strength is of order 100 MPa but that faults are brittle and generate little heat because they lose essentially all of that strength in very small slip. If stress equaled that strength over the entire fault plane, and the strength drop was total, the displacement would be of order 50 m. That will, however, be an irrelevant number for actual earthquakes if the fault has some combination of defect regions of much lower effective stress, which act like Griffith cracks in nucleating ruptures, or if the fault retains severe local stress concentrations from previously stopped events or from stressing at borders between locked and creeping zones. Then the peak strength can be irrelevant to the average stress level at which the fault operates, which is instead the stress at which a rupture nucleated at one of those easy spots can propagate over large distances. Thus the characteristic slip in an actual event is properly chosen as that associated with dropping that propagation stress level to zero.

The weakening state variable Q', and also the characteristic weakening distances $1/\alpha'$ (not to be confused with α' in the body of the text) and $1/\beta'$ relate to their dimensionless equivalents just as U' does to U. Thus $\alpha = 3$ corresponds in the strike-slip example to a characteristic large scale slip-weakening distance $1/\alpha' = 0.5$ m.

The plate loading rate $\nu' = \nu c\Delta\Phi/(G(1 + \sigma))$ corresponds in the strike-slip case, with $\nu = 0.0001$, to $9 \cdot 10^{-5}$ m/s for the strength drop 10 MPa mentioned. This is many of orders of magnitude faster than typical plate rates, around 10^{-9} m/s, or 30 mm/a, but much slower than seismic slip rates. Also, the characteristic time for relaxation of the state parameter Q' back towards its pre-weakening value of 0 is $1/\gamma' = W/(c\gamma)$. This is about 50 s in the strike-slip case for a typical $\gamma = 0.1$, such as we use in the slip weakening range which is the primary focus here. It would be about 0.5 s for $\gamma = 10$ which would be in the velocity weakening range. Finally, the Langer viscous parameter, multiplying the second gradient of slip rate, is $\eta' = \eta W^2 G/c$. For $\eta = 10^{-5}$ as in the examples here, this is $\eta' = 2.3 \cdot 10^4$ MPa-m-s in the strike slip case.

Appendix B: Stabilizing the Small Scales With the Viscous Term

For nonzero γ the dispersion relation (13) is modified slightly, and we get, effectively, an extra velocity weakening term which scales with γ. This can be seen as follows. Using the integral formulation for Q (equation (9)), restricting ourselves to positive slip rates, we integrate by parts:

$$Q(t) = \int_{-\infty}^{t} e^{-\gamma(t-t')} \frac{\partial S}{\partial t'} dt' = S - \gamma \int_{-\infty}^{t} e^{-\gamma(t-t')} S dt' . \tag{B1}$$

Now using the sinusoidal form for the motion S (equation (12)), we replace the slip S in the integral by $1/\Omega$ times the slip rate:

$$Q(t) = S - \frac{\gamma}{\Omega} \int_{-\infty}^{t} e^{-\gamma(t-t')} \frac{\partial S}{\partial t'} dt' . \tag{B2}$$

Equating the middle equation in (B1) with the right-hand side of (B2) and then collecting terms, we get

$$\int_{-\infty}^{t} e^{-\gamma(t-t')} \frac{\partial S}{\partial t'} dt' = \frac{S}{1 + \gamma/\Omega} = Q . \tag{B3}$$

Since when $\gamma = 0$ we have $Q = S$, we find that the nonzero γ effectively renormalizes the slip weakening rate $\hat{\alpha}$ to $\hat{\alpha}/(1 + \gamma/\Omega)$; that is, it picks up a velocity weakening part (the $1/\Omega$ piece).

To examine the stability in this nonzero γ case, we plug the renormalized $\hat{\alpha}/(1 + \gamma/\Omega)$ into our dispersion relation (13), and generalize to nonzero η to get

$$(\Omega^2 + k^2 + 1)^{1/2} = \frac{\hat{\alpha}}{1 + \gamma/\Omega} - \eta k^2 \Omega . \tag{B4}$$

Looking at small values of γ and η and linearizing for small γ/Ω, an approximation which is valid away from the critical wavelength $\hat{x}$ where $\Omega = 0$, we can solve this equation perturbatively about the $\gamma = 0$ and $\eta = 0$ solution to first order in γ and η. This will show us how our dispersion relation is stabilized at small wavelengths. Taking (B4), squaring, and keeping only lowest-order γ and η terms gives

$$\Omega^2 + k^2 + 1 = \hat{\alpha}^2(1 - 2\gamma/\Omega) - 2\hat{\alpha}\eta k^2 \Omega + O(\gamma^2, \eta^2, \gamma\eta) , \tag{B5}$$

or, rearranging terms,

$$\Omega = \sqrt{\hat{\alpha}^2 - k^2 - 1 - \frac{2\gamma\hat{\alpha}^2}{\Omega} - 2\hat{\alpha}\eta k^2 \Omega + O(\gamma^2, \eta^2, \gamma\eta)} . \tag{B6}$$

Defining $\Omega_0 \equiv \sqrt{\hat{\alpha}^2 - k^2 - 1}$ which is Ω when $\gamma = \eta = 0$ as in equation (13), as long as we are away from $\Omega_0 = 0$, we can replace Ω on the right-hand side by Ω_0, since the right-hand side Ω terms are already of order $O(\gamma, \eta)$. Thus, away

from $\Omega_0 = 0$, expanding the square root the result is the dispersion relation

$$\Omega = \pm i\sqrt{k^2 + 1 - \hat{\alpha}^2} + \left(\frac{\hat{\alpha}^2\gamma}{k^2 + 1 - \hat{\alpha}^2} - \hat{\alpha}\eta k^2\right) + O(\gamma^2, \eta^2, \gamma\eta)\,. \quad \text{(B7)}$$

Here we see now the utility of the η term, which stabilizes the large k.

Acknowledgments. Raul Madariaga and Jim Langer provided helpful comments on the manuscript, and Nadia Lapusta provided both comments and supplementary calculations with rate and state constitutive laws to examine some of the issues discussed. B.E.S. was supported by NSF grants EAR-94-17700 and EAR-99-09287 and USGS grant 1434-HQ-97-GR-O3074. J.R.R. was supported by the Southern California Earthquake Center (SCEC), USGS grants 1434-HQ-97-GR-03094 and 99-HQ-GR-0025, and by a Blaise Pascal Chair of the Foundation of Ecole Normale Superieure, Paris. SCEC is supported by NSF Cooperative Agreement EAR-8920136 and USGS Cooperative Agreement 1434-HQ-97-AG-01718.

References

Aki, K., and P. Richards, *Quantitative Seismology: Theory and Methods*, W.H. Freeman, New York, 1980.

Alford, R.M., K.R. Kelly, and D.M. Boore, Accuracy of finite difference modeling of the acoustic wave equation, *Geophysics, 36*, 834, 1974.

Andrews, D.J., Rupture propagation with finite stress in antiplane strain, *J. Geophys. Res., 81*, 3575, 1976.

Ben-Zion, Y., and J.R. Rice, Earthquake failure sequences along a cellular fault zone in a three-dimensional elastic solid containing asperity and nonasperity regions, *J. Geophys. Res., 98*, 14,109, 1993.

Ben-Zion, Y., and J.R. Rice, Slip patterns and earthquake populations along different classes of faults in elastic solids *J. Geophys. Res., 100*, 12,959, 1995.

Ben-Zion, Y., and J.R. Rice, Dynamic simulations of slip on a smooth fault in an elastic solid *J. Geophys. Res., 102*, 17,771, 1997.

Blanpied, M.L., T.E. Tullis, and J.D. Weeks, Frictional behavior of granite at low and high sliding velocities, *Geophys. Res. Lett., 14*, 554, 1987.

Blanpied, M.L., D.A. Lockner, and J.D. Byerlee, Fault stability inferred from granite sliding experiments at hydrothermal conditions, *Geophys. Res. Lett., 18*, 609, 1991.

Brace, W.F., and J.D. Byerlee, Stick-slip as a mechanism for earthquakes, *Science, 153*, 990, 1966.

Burridge, R., and L. Knopoff, Model and theoretical seismicity, *Bull. Seismol. Soc. Am., 57*, 341, 1967.

Carlson, J.M., and J.S. Langer, Mechanical model of an earthquake fault, *Phys. Rev. A, 40*, 6470, 1989.

Carlson, J.M., J.S. Langer, B.E. Shaw, and C. Tang, Intrinsic properties of a Burridge-Knopoff model of an earthquake fault, *Phys. Rev. A, 44*, 884-897, 1991.

Cochard, A., and R. Madariaga, Complexity of seismicity due to highly rate-dependent friction, *J. Geophys. Res., 101*, 25,331, 1996.

Davison, F.C., and C.H. Scholz, Frequency-moment distribution of earthquakes in the Aleutian Arc: A test of the characteristic earthquake model, *Bull. Seismol. Soc. Am., 75*, 1349, 1985.

Day, S.M., Three-dimensional simulation of spontaneous rupture: The effect of non-uniform prestress, *Bull. Seismol. Soc. Am., 72*, 1881, 1982.

Dieterich, J.H., Modeling of rock friction, 1, Experimental results and constitutive equations, *J. Geophys. Res., 84*, 2161, 1979.

Dieterich, J.H., Earthquake nucleation and faults with rate- and state-dependent strength, *Tectonophysics, 211*, 115, 1992.

Gu, J.C., J.R. Rice, A.L. Ruina, and S.T. Tse, Slip motion and stability of a single degree of freedom elastic system with rate and state dependent friction *J. Mech. Phys. Solids, 32*, 167, 1984.

Gutenberg, B., and C.F. Richter, *Seismicity of the Earth and Related Phenomena*, Princeton Univ. Press, Princeton, N. J., 1954.

Heslot, F., T. Baumberger, B. Perrin, B. Caroli, and C. Caroli, Creep, stick-slip, and dry-friction dynamics– Experiments and a heuristic model, *Phys. Rev. E, 49*, 4973, 1994.

Horowitz, F.G., and A. Ruina, Slip patterns in a spatially homogeneous fault model, *J. Geophys. Res., 94*, 10,279, 1989.

Ida, Y., Stress concentrations and unsteady propagation of longitudinal shear cracks, *J. Geophys. Res., 78*, 3419, 1973.

Johnson, E., The influence of the lithospheric thickness on bilateral slip, *Geophys. J. Int., 108*, 151, 1992.

Kostrov, B.V., and S. Das, *Principles of Earthquake Source Mechanics*, Cambridge Univ. Press, New York, 1988.

Lachenbruch, A., Frictional heating, fluid pressure, and the resistance to fault motion, *J. Geophys. Res., 85*, 6097, 1980.

Langer, J.S., and H. Nakanishi, Models of rupture propagation II: Two dimensional model with dissipation on the fracture surface, *Phys. Rev. E, 48*. 439, 1993.

Langer, J.S., J.M. Carlson, C.H. Myers, and B.E. Shaw, Slip complexity in dynamic models of earthquake faults, *Proc. Natl. Acad. Sci. U.S.A., 93*, 3825, 1996.

Lapusta, N. and J.R. Rice, Elastodynamic simulations of earthquake sequences in a 2D model of a faulted plate coupled to a moving substrate, *Eos Trans. AGU, 78* (46), Fall Meet. Suppl., F449, 1997.

Lapusta, N. and J.R. Rice, Complex multi-pulse mode of rupture propagation, *Eos Trans. AGU, 79* (45), Fall Meet. Suppl., F662, 1998.

Lehner, F.K., V.C. Li, and J.R. Rice, Stress diffusion along rupturing plate boundaries, *J. Geophys. Res., 86*, 6155, 1981.

Madariaga, R., Dynamics of an expanding circular crack, *Bull. Seismol. Soc. Am., 66*, 639, 1976.

Mase, C.W., and L. Smith, Effects of frictional heating on the thermal, hydrologic, and mechanical response of a fault, *J. Geophys. Res., 92*, 6249, 1987.

Myers, C.R., B.E. Shaw, and J.S. Langer, Slip complexity in a two dimensional crustal plane model, *Phys. Rev. Lett., 77*, 972, 1996.

Nielsen, S., L. Knopoff, and A. Tarantola, Model of earthquake recurrence: Role of elastic wave radiation, relaxation of friction, and inhomogeneity, *J. Geophys. Res., 100*, 12,423, 1995.

Okubo, P., and J.H., Dieterich, Effects of physical fault properties on frictional instabilities produced on simulate faults, *J. Geophys. Res., 89*, 5815, 1984.

Olsen, K. B., R. Madariaga, and R.J. Archuleta, Three dimensional dynamic simulation of the 1992 Landers earthquake, *Science, 278*, 834, 1997.

Pacheco, J.F., C.H. Scholz, and L.R. Sykes, Changes in frequency size relationship from small to large earthquakes, *Nature, 355*, 71-3, 1992.

Rice, J.R., The mechanics of earthquake rupture, in *Physics of the Earth's Interior* (Proc. Int. Sch. of Phys. Enrico Fermi, 78, edited by A.M. Dziewonski and E. Boschi, pp. 555-649, North-Holland, New York, 1980.

Rice, J.R., Spatiotemporal complexity of slip on a fault, *J. Geophys. Res., 98*, 9885, 1993.

Rice, J.R., Earthquakes at low driving stress in a high strength, low toughness fault zone: Shear-heating example, *Eos Trans. AGU, 75* (44), Fall Meet. Suppl., F426, 1994.

Rice, J.R. Low stress faulting: Strong but brittle faults with local stress concentrations, *Eos Trans. AGU, 77* (46), Fall Meet. Suppl., F471, 1996.

Rice, J.R., and Y. Ben-Zion, Slip complexity in earthquake fault models, *Proc. Natl. Acad. Sci. U.S.A., 93*, 3811, 1996.

Rice, J.R., and A. Ruina, Stability of steady frictional sliding, *J. Appl. Mech., 50*, 343, 1983.

Ruina, A., Slip instability and state variable friction laws, *J. Geophys. Res., 88*, 10,359, 1983.

Schwartz, D.P., and K.J. Coppersmith, Fault behavior and characteristic earthquakes: Examples from the Wasatch and San Andreas fault zones, *J. Geophys. Res., 89*, 5681, 1984.

Shaw, B.E., Moment spectra in a simple model of an earthquake fault, *Geophys. Res. Lett., 20*, 643, 1993.

Shaw, B.E., Complexity in a spatially uniform continuum fault model, *Geophys. Res. Lett., 21*, 1983, 1994.

Shaw, B.E., Frictional weakening and slip complexity on earthquake faults, *J. Geophys. Res., 100*, 18,239, 1995.

Shaw, B.E., Modelquakes in the two dimensional wave equation, *J. Geophys. Res., 102*, 27,367, 1997.

Shaw, B.E., Far field radiated energy scaling in elastodynamic earthquake fault models, *Bull. Seismol. Soc. Am., 88*, 1457, 1998.

Shaw, B.E., J.M. Carlson, and J.S. Langer, Patterns of seismic activity preceding large earthquakes, *J. Geophys. Res., 97*, 479, 1992.

Sibson, R.H., Interactions between temperature and pore fluid pressure during earthquake faulting and a mechanism for partial or total stress relief, *Nature, 243*, 66, 1973.

Singh, S., M. Rodriguez, and L. Esteva, Statistics of small earthquakes and frequency of occurrence of large earthquakes along the Mexican subduction zone, *Bull. Seismol. Soc. Am., 73*, 1779, 1983.

Sipkin, S.A., and T.H. Jordan, Frequency dependence of Q_{ScS}, *Bull. Seismol. Soc. Am., 69*, 1055, 1979.

Tse, S., and J.R. Rice, Crustal earthquake instability in relation to the depth variations of frictional slip properties, *J. Geophys. Res., 91*, 9452, 1986.

Virieux, J. and R. Madariaga, Dynamic faulting studied by a finite difference method, *Bull. Seismol. Soc. Am., 72*, 345, 1982.

Wesnousky, S.G., C.H. Scholz, K. Shimazaki, and T. Matsuda, Earthquakes frequency distribution and the mechanics of faulting, *J. Geophys. Res., 88*, 9331, 1983.

Zheng, G., and J.R. Rice, Conditions under which velocity-weakening friction allows a self-healing versus crack-like mode of rupture, *Bull. Seismol. Soc. Am., 88*,, 1466, 1998.

J. R. Rice, Department of Earth and Planetary Sciences and Division of Engineering and Applied Sciences, Harvard University, Cambridge, MA, 02138. (rice@esag.harvard.edu)

B. E. Shaw, Lamont-Doherty Earth Observatory, Columbia University, Palisades, NY 10964. (shaw@ldeo.columbia.edu)

(Received May 21, 1999; revised February 21, 2000;
accepted June 5, 2000.)